

DIETBORNE BIOAVAILABILITY OF COPPER FROM COBBLE COATINGS IN A
MINING-INFLUENCED STREAM: THE EFFECT OF ORGANISM (*L. STAGNALIS*)
MASS ON REVERSE ISOTOPE LABELING MEASUREMENTS

By
Jill Murphy

A thesis submitted to the Faculty and the Board of Trustees of the Colorado School of Mines in partial fulfillment of the requirements for the degree of Master of Science (Geochemistry).

Golden, CO

Date _____

Signed: _____
Jill K. Murphy

Signed: _____
Dr. James F. Ranville
Thesis Advisor

Golden, CO

Date _____

Signed: _____
Dr. Thomas Gennett
Professor and
Department Head of Chemistry

ABSTRACT

The legacy impacts of hardrock mining are complex and difficult to fully mitigate. Though the detrimental effects of hardrock mining on environmental quality have been extensively researched, there is a paucity of data documenting the temporal responses of mining influenced waterways (MIW) to remediation efforts. In an effort to bridge this information gap, I examined the bioavailability of copper (Cu) present in armored metal-oxyhydroxide cobble coatings collected before and after the completion of a high-density-sludge lime treatment plant on the North Fork of Clear Creek (NFCC) in Black Hawk, Gilpin County, Colorado. Using an innovative reverse-labeling stable-isotope method developed by U.S. Geological Survey researchers, I calculated Cu assimilation efficiency (AE) in freshwater snails (*Lymnaea stagnalis*) that were fed cobble-coating particles.

Although Cu bioavailability did not differ significantly between pre- and post-remediation metal-oxyhydroxide particles (~34% AE), high among-replicate variability resulted in low power to infer statistically significant differences. The use of small organisms (~0.5-5 mg dry tissue weight) in early post-embryonic ontogeny may have contributed to the relatively high variability, which may be related to uncertainty in the estimation of differences in tissue Cu concentrations between exposed and background snails. A novel finding was that background Cu concentrations decreased with increasing size, following the relationship: $[^{63}\text{Cu}]_{\text{snail}} = 70.088 \times M_{\text{snail}}^{-0.628}$, where the units for $[^{63}\text{Cu}]_{\text{snail}}$ are $\text{mg } ^{63}\text{Cu g}_{\text{snail}}^{-1}$ and the units for M_{snail} are mg. These size constraints may have important implications for the planned adaptation of this method to smaller benthic organisms that are more ecologically relevant in high-gradient, montane streams (e.g., the midge *Chironomus dilutus*). Further work is needed to determine

whether organism size, growth rate, or developmental stage is the primary source of among-replicate variability.

TABLE OF CONTENTS

ABSTRACT	iii
LIST OF FIGURES	viii
LIST OF TABLES	x
LIST OF SYMBOLS	xi
ACKNOWLEDGEMENTS	xv
CHAPTER 1 INTRODUCTION	1
1.1 Acid mine drainage and the environment	1
1.2 Cobble coatings in mining influenced waters	2
1.3 The need for temporal assessments of remediation efficacy	4
1.4 Reverse isotopic labeling as a measure of copper bioavailability	6
1.5 History of mining and remediation on North Fork Clear Creek	8
1.6 Thesis objectives	11
1.7 References	12
CHAPTER 2 DIETBORNE BIOAVAILABILITY OF COPPER IN ACID MINE DRAINAGE-RELATED PARTICLES TO FRESHWATER SNAILS (<i>LYMNAEA STAGNALIS</i>), AND THE IMPORTANCE OF ORGANISM SIZE IN A REVERSE-LABELING STABLE-ISOTOPIC METHOD	17
2.1 Abstract	17
2.2 Introduction	18
2.3 Methods	20
2.3.1 Collection, preparation, and characterization of armored metal oxyhydroxide cobble coatings from North Fork Clear Creek	20

2.3.1.1	Cobble collection and preparation of cobble coatings.....	20
2.3.1.2	X-ray diffraction	23
2.3.1.3	VP-SEM and TIMA3	23
2.3.1.4	Analyses of armored cobble coating copper content.....	24
2.3.2	Copper bioavailability experiments	25
2.3.2.1	Materials preparation	25
2.3.2.2	Test organisms	25
2.3.2.3	Isotopic reversal and dietborne exposures	25
2.3.2.4	Sample preparation and chemical analyses.....	28
2.3.2.5	Data analysis	29
2.4	Results and discussion	32
2.4.1	Cobble coatings.....	32
2.4.1.1	X-ray diffraction	32
2.4.1.2	VP-SEM and TIMA3	33
2.4.2	Organism size analyses	33
2.4.3	Copper bioavailability pre- and post-remediation	47
2.5	Synthesis	50
2.6	Acknowledgements.....	54
2.7	References.....	54
CHAPTER 3	SUMMARY AND CONCLUSIONS	57
3.1	Summary of results and implications.....	57

3.2	Recommendations for future research	59
3.3	References.....	61
APPENDIX A: SUPPLEMENTAL INFORMATION.....		62

LIST OF FIGURES

Figure 1.1	Illustrative graph showing $^{65/63}\text{Cu}$ ratios in snail tissues decreasing with increasing exposure to Cu-containing natural particles.....	7
Figure 1.2	Photograph of the Gregory Diggings in Central City, CO, 1859 or 1860.....	9
Figure 1.3	Photograph of tailings piles and wasterock at the Gilpin-Eureka Mine, CO, 1819.....	9
Figure 2.1	Map of the North Fork of Clear Creek.....	21
Figure 2.2	Diffraction pattern from an oriented aggregate mount prepared from the < 2 mm size fraction of armored cobble coatings removed from North Fork Clear Creek cobble collected in February 2017.....	34
Figure 2.3	Diffraction pattern from an oriented aggregate mount prepared from the < 2 μm size fraction of armored cobble coatings removed from North Fork Clear Creek cobble collected in February 2017.....	34
Figure 2.4	Diffraction pattern from an oriented aggregate mount prepared from the < 2 mm size fraction of armored cobble coatings removed from North Fork Clear Creek cobble collected in August 2017.....	35
Figure 2.5	Diffraction pattern from an oriented aggregate mount prepared from the < 2 μm size fraction of armored cobble coatings removed from North Fork Clear Creek cobble collected in August 2017.....	35
Figure 2.6	Qualitative element map of Fe (K family) dispersal in armored cobble coatings collected in February 2017	36
Figure 2.7	Qualitative element map of Si (K family) dispersal in armored cobble coatings collected in February 2017	37
Figure 2.8	Qualitative element map of Fe (K family) dispersal in armored cobble coatings collected in August 2017	38
Figure 2.9	Qualitative element map of Si (K family) dispersal in armored cobble coatings collected in August 2017	39
Figure 2.10	Visual monitoring results at the Above Russell Gulch (ARG) site in March 2017 and August 2017.....	40

Figure 2.11	^{63}Cu accumulated by <i>L. stagnalis</i> calculated using the average of $[\text{}^{63}\text{Cu}]_{\text{snail}}$ values measured in “background” snails	41
Figure 2.12	Concentrations of ^{63}Cu in soft tissue of <i>L. stagnalis</i>	43
Figure 2.13	^{63}Cu accumulated by <i>L. stagnalis</i> calculated using size-specific $[\text{}^{63}\text{Cu}]_{\text{b,snail}}$ values	45
Figure 2.14	Background concentrations of ^{65}Cu in soft tissue of <i>L. stagnalis</i>	46
Figure 2.15	Concentrations of total Cu in soft tissue of <i>L. stagnalis</i>	47
Figure 2.16	Background ratios of ^{65}Cu to ^{63}Cu in <i>L. stagnalis</i> not exposed to North Fork Particles (NFP).....	48
Figure 2.17	$^{65}\text{Cu}:\text{}^{63}\text{Cu}$ measured in <i>L. stagnalis</i> exposed to mixtures of diatoms and armored cobble coating particles removed from North Fork Clear Creek (NFCC) cobble collected in February 2017 (pre-remediation) and August 2017 (post-remediation)	49
Figure 2.18	Assimilation efficiency (AE) of ^{63}Cu by <i>L. stagnalis</i> exposed to mixtures of diatoms and armored cobble coating particles removed from North Fork Clear Creek (NFCC) cobble collected in February 2017 (pre-remediation) and August 2017 (post-remediation) calculated using fixed averages of background ^{63}Cu concentrations measured in <i>L. stagnalis</i>	50
Figure 2.19	Assimilation efficiency (AE) of ^{63}Cu by <i>L. stagnalis</i> exposed to mixtures of diatoms and armored cobble coating particles removed from North Fork Clear Creek (NFCC) cobble collected in February 2017 (pre-remediation) and August 2017 (post-remediation) re-calculated using size-specific $[\text{}^{63}\text{Cu}]_{\text{b,snail}}$	51
Figure A.1	Assimilation efficiency (AE) of ^{63}Cu by <i>L. stagnalis</i> exposed to mixtures of diatoms and armored cobble coating particles removed from North Fork Clear Creek (NFCC) cobble collected in May 2017	70
Figure A.2	Assimilation efficiency (AE) of ^{63}Cu by <i>L. stagnalis</i> exposed to mixtures of diatoms and armored cobble coating particles removed from North Fork Clear Creek (NFCC) cobble collected in August 2017	71
Figure A.3	^{63}Cu accumulated over a 4-hour exposure period from loose cobble coatings removed from North Fork Clear Creek (NFCC) cobble collected in May 2017 vs. organism dry tissue mass (mg)	72

LIST OF TABLES

Table 2.1	Volumes of North Fork Particle Suspensions (NFPS) and masses of diatoms used to create diatom-NFP feeding mats.....	27
Table 2.2	Parameters used to calculate the total mass of ^{63}Cu (ng) accumulated from armored metal-oxyhydroxide cobble coatings in North Fork Particle Suspensions (NFPS) and Cu assimilation efficiency by <i>L. stagnalis</i> over a 4-hour exposure period.....	30
Table A.1	Summary of data used to determine Cu bioavailability in <i>L. stagnalis</i>	62
Table A.2	Size-specific pre-exposure tissue concentrations of ^{63}Cu in <i>L. stagnalis</i> ($[\text{}^{63}\text{Cu}]_{\text{b,snail}}$) calculated using the equation of the curve fit to measured $[\text{}^{63}\text{Cu}]_{\text{snail}}$ in “background” snails, and the difference between size-specific values and the average of all measured $[\text{}^{63}\text{Cu}]_{\text{snail}}$ in “background” snails ($\overline{[\text{}^{63}\text{Cu}]_{\text{b}}}$).....	65
Table A.3	Summary of water chemistry measured in the field and analytically on both cobble sampling dates (February 2, 2017 and August 29, 2017) at the Railless Below Plant (RBP) site	66

LIST OF SYMBOLS

Acid Mine Drainage	AMD
Arsenic	As
Assimilation efficiency	AE
Average background concentration of copper 63 in snail soft tissue	$\overline{[^{63}\text{Cu}]_b}$
Average copper 63 in snails exposed to diatoms only	$\overline{[^{63}\text{Cu}]_d}$
Back-calculated background concentration of copper 63 in snail soft tissue	$[^{63}\text{Cu}]_{0,\text{snail}}$
Before-and-after control-impact	BACI
Cadmium	Cd
Chloride ion	Cl ⁻
Cobalt	Co
Colorado Department of Public Health and Environment	CDPHE
Concentration of copper 63 in lettuce	$[^{63}\text{Cu}]_{\text{lett}}$
Concentration of copper 63 in North Fork particles	$[^{63}\text{Cu}]_{\text{NFP}}$
Concentration of copper 63 in snail soft tissue	$[^{63}\text{Cu}]_{\text{snail}}$
Copper	Cu
Copper 63 accumulated over the exposure period	$^{63}\text{Cu}_{\text{accumulated}}$
Copper 63 isotope	^{63}Cu
Copper 65 isotope	^{65}Cu
Copper k(alpha) radiation	Cu-Kα
Counts per second	cps
Day(s)	d

Degrees Celsius	°C
Deionized	DI
Dissolved organic carbon	DOC
Dissolved organic matter	DOM
Duration of the exposure period	T ₁
Duration of the depuration period	T ₂
Ferric iron	Fe ³⁺
Ferrous iron	Fe ²⁺
Gram	g
High-density sludge	HDS
Hour	h
Hydrogen ion	H ⁺
Hydrogen peroxide	H ₂ O ₂
Hydroxide ion	OH ⁻
Inductively coupled plasma-atomic emission spectroscopy	ICP-AES
Inductively coupled plasma-mass spectrometry	ICP-MS
Ingestion rate	IR
Iron	Fe
Kilometer	km
Lead	Pb
Liter	L
<i>Lymnaea stagnalis</i>	<i>L. stagnalis</i>
Measured background concentration of copper 63 in snail soft tissue	[⁶³ Cu] _{b,snail}

Microgram	μg
Microliter	μl
Micrometer	μm
Milligram	mg
Milliliter	ml
Millimeter	mm
Mining influenced waters	MIW
Minute(s)	min
Moderately hard reconstituted water	MHRW
Month(s)	mo(s)
National Institute of Standards and Technology	NIST
Nickel	Ni
Nitric acid	HNO_3
North Fork of Clear Creek	NFCC
North Fork particles	NFP
North Fork particle suspension	NFPS
Railless Below Plant	RBP
Rate constant of copper uptake from feeding mat	$k_{u,mat}$
Rate constant of copper uptake from lettuce	$k_{u,lett}$
Rate of loss of copper	k_e
Rotations per minute	rpm
Standard deviation	SD
Sulfate ion	SO_4^{2-}

Total organic carbon	TOC
United States Bureau of Land Management	BLM
United States Environmental Protection Agency	USEPA
X-ray diffraction	XRD
Zinc	Zn

ACKNOWLEDGEMENTS

First and foremost, I would like to thank my advisor, Professor James F. Ranville, without whose guidance, insight, and humor the completion of this Master's Thesis would not have been possible. Thank you for lending your time, funding, support, and endless knowledge throughout this process.

Next I would like to extend my sincere thanks to Dr. Joseph S. Meyer, who raised questions I had not even begun to consider at every twist and turn of my research journey. Your challenging inquisitions and meticulous edits helped propel me to new heights as a scientist and a writer.

Without the support and input of my final two committee members, Professors Alexis Navarre-Sitchler and Junko Munakata-Marr, the organization and completion of this work would certainly not have been possible. Thank you for your guidance and insight.

I would also like to acknowledge all of the members of the Ranville research group, without whom I would almost certainly not have been able to withstand the pressures of graduate school. Specifically, I would like to thank Dr. Ellie Traudt for your friendship and mentorship, and Katie Challis for being a great friend and for working around my bizarre schedule to rescue many of my ICP-MS runs at all sorts of odd hours.

Lastly, I would be remiss if I did not acknowledge my family's tremendous role in my completing this chapter of my life. To my parents, my siblings, and my fiancé, thank you all from the bottom of my heart for being there to lift me up when the challenges presented by my pursuit of a career in science seemed insurmountable.

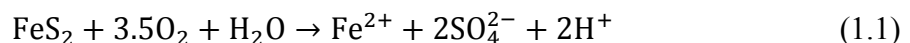
CHAPTER 1

INTRODUCTION

1.1 Acid mine drainage and the environment

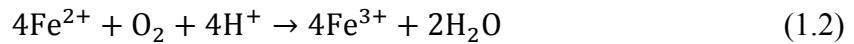
The hardrock mining industry has long been hailed as a cornerstone in the development of the modern American economy and the settlement of the American West. In spite of these positive economic impacts, the industry has a dismal environmental legacy, having left in its wake innumerable abandoned mineshafts and myriad contaminated bodies of freshwater. Under the General Mining Law of 1872, which was passed to promote mineral exploration on public lands, a mining claim could simply be abandoned once it was deemed to no longer be profitable.¹ Consequently, current reports estimate that there are anywhere between 160,000 and 557,000 abandoned mines in the United States,^{2,3} with nearly 11,000 of those in Colorado.⁴ Once abandoned, mining tunnels bored into mountainsides, and the waste rock excavated from their depths, continue to be exposed to molecular oxygen (O₂) and water. Many of the precious metals responsible for the western United States mining boom are commonly associated with iron sulfide minerals [e.g., pyrite (FeS₂)], which, when oxidized in the presence of O₂ and water, generate an acidic, metal-rich effluent called acid mine drainage (AMD).

The first stage of AMD generation comprises the exposure of iron sulfide minerals to O₂ and water, producing soluble ferrous iron (Fe²⁺), sulfate (SO₄²⁻), and hydrogen (H⁺) ions (Equation 1.1).

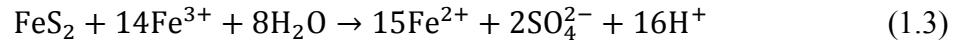


The overall oxidation of sulfide in the iron is coupled with the reduction of ferric iron (Fe³⁺) to Fe²⁺. Because Fe³⁺ is a more effective oxidant for metal sulfides than O₂, the remainder

of the reaction pathway proceeds first with the oxidation of Fe^{2+} to Fe^{3+} coupled with the reduction of O_2 to water (Equation 1.2),



and then with the oxidation of iron sulfides, coupled with the reduction of Fe^{3+} to Fe^{2+} (Equation 1.3).



The resulting acidic effluent leaches additional metals that are solubilized under acidic conditions from the surrounding rock. These metals can include arsenic (As), cadmium (Cd), copper (Cu), lead (Pb), nickel (Ni), and zinc (Zn), all of which can cause toxicity in aquatic organisms.⁵⁻¹⁰

Although the products of AMD generation are concerning, the geochemical reactions governing the process occur relatively slowly in abiotic systems. In most mining-influenced environments, however, acidophilic chemoautotrophic bacteria and archaea thrive in the subsurface, increasing metal sulfide oxidation rates many-fold.¹¹ Consequently, an estimated 40% of American headwaters are currently contaminated with AMD.¹² Bodies of water with chemistry that has been altered by mining activities or AMD contamination are more broadly categorized as mining-influenced waters (MIW), to acknowledge that not all MIW are low pH.¹³

1.2 Cobble coatings in mining influenced waters

One of the signature characteristics of MIW is the presence of ochre-colored metal oxide coatings on streambed cobble. The exact composition and mineralogy of the metal oxide coatings in and across any given mining-influenced system can vary considerably, depending on the metals in AMD entering the system, the streambed and surrounding bedrock mineralogy,

stream pH and alkalinity, the presence of mixing zones, and the presence or absence of dissolved organic matter (DOM).¹⁴

AMD is generally metal-rich due to the favorability of acidic conditions for trace metal mobilization (dissolution and/or desorption) and transport.¹⁵⁻¹⁷ Because iron sulfide minerals (e.g., pyrite and pyrrhotite) are the predominant sulfidic minerals in most hard rock mining environments,¹⁸ iron (Fe) is one of the most abundant metals found in AMD. The primary control on iron solubility is pH, with Fe (III) being soluble below a pH of ~3.2 and insoluble above that pH.¹⁴ As AMD mixes with non-impacted freshwater, pH usually increases to a circumneutral range (i.e., ~6.0 < pH < ~8.0). Under circumneutral conditions, Fe²⁺ iron very rapidly oxidizes to Fe³⁺, which then hydrolyzes to form insoluble metal-oxyhydroxide nanoparticles. The resulting nanoparticles can then undergo oriented aggregation,¹⁹ forming metal-oxyhydroxide complexes of varying degrees of hydration and crystallinity.^{19,20} These solids then accumulate on cobble surfaces, resulting in a loose, flocculent coating ranging in color from red-orange to yellow. Over time, the floc may begin to form an armored coating featuring poorly crystalline metal-oxyhydroxide minerals. The resulting mineral phases in the armored coating depend on stream pH and anion species present in solution.¹⁹ Under acidic conditions, metal-oxyhydroxides in solutions that contain sufficient concentrations of chloride ion (Cl⁻) and sulfate ion (SO₄²⁻), which form strong bonds with Fe³⁺, may form akaganeite [Fe³⁺O(OH,Cl)] or schwertmannite [Fe³⁺₁₆O₁₆(SO₄)₂(OH)₁₂ • nH₂O].¹⁹ In circumneutral waters, Fe³⁺ complexation with OH⁻ is favored over all other anions, causing ferrihydrite [5Fe₂O₃ • 9H₂O] to be the dominant observed mineral phase.¹⁹ Finally, in solutions containing phosphate (PO₄³⁻) or silicate (SiO₄⁴⁻), which form very strong bonds with Fe³⁺, metal-oxyhydroxide particles might not form at all.^{21,22}

Because metal-oxyhydroxide particles are dynamic sorbents in metal-rich solutions, cobble coatings in MIW typically feature high concentrations of trace metals in addition to Fe. The extent of sorption of a given trace metal to metal-oxyhydroxide cobble coatings in MIW can vary drastically, depending on the trace metal, the degree of crystallinity and mineralogy of the cobble coatings, and solution pH and composition. Copper, for example, sorbs more effectively to poorly crystalline, metal-oxyhydroxide-sulfate complexes than to schwertmannite at $\text{pH} < 6.5$, but sorbs equally effectively to both mineral phases at $\text{pH} > 6.5$.²³

1.3 The need for temporal assessments of remediation efficacy

Although much research has been performed on the mechanisms of AMD generation and its environmental impacts, little work has been done to document the responses of MIW-influenced streams to remediation. In general, remediation of mine sites involves removal of the sources of acidity and metals. In particular, these sources include solid wastes (tailings and waste rock) and effluents from tunnels and adits.²⁴ Chemical and biological recovery of the streambed primarily occurs by natural processes.²⁵ In MIW undergoing remediation, metals in cobble coatings may be removed from the streambed by dissolution, desorption, and/or mechanical scouring.²⁶ Although mechanical scouring occurs annually (e.g., during spring runoff in montane streams), the process does not permanently eliminate metal-rich cobble coatings until a supplemental remediation system operates to eliminate the source of AMD. Otherwise, coatings will continue to accumulate seasonally.

In 2008, Ross et al.²⁷ compared benthic macroinvertebrate communities in limestone streams (alkaline streams with limestone lithology) and freestone streams (circumneutral streams fed by snow melt or rain with sandstone, shale, crystalline lithology) with and without sources of AMD. While not directly related to an extant MIW remediation project, the researchers

identified benthic macroinvertebrate community parameters (e.g., density, diversity, taxa richness) and indicator species that could be used to evaluate the impacts of limestone-based remediation on benthic macroinvertebrate communities in MIW. Results of the work identified several taxa, including the genera *Neophylax*, *Drunella*, and *Gammarus*, that could be used as significant indicators of recovery in limestone and freestone systems. Additionally, the study identified trophic and functional differences in benthic communities in limestone-buffered and freestone streams with and without AMD that could be used to evaluate remediation progress in the absence of the indicator species.

Clements et al.²⁸ expanded on this type of work in 2010 with the publication of one of the most comprehensive studies of physicochemical and biological data for MIW to date. The study comprised 17 years of seasonal and annual measurements of water quality, metal concentrations in cobble, macroinvertebrate communities, and brown trout populations before and after several stages of restoration and remediation (e.g., removal of mine tailings, installation of water treatment facilities, and revegetation of riparian areas) on the Arkansas River near Leadville, Colorado. Remediation success varied seasonally, spatially, and among response variables. Additionally, the authors reported that the determination of whether or not MIW have recovered following treatment is further complicated by potential differences in recovery rates of cobble and the water column.

More recently, Mebane et al.²⁹ published results of a 30-year study examining stream communities impacted by the Blackbird Mine in central Idaho before, during, and after water quality restoration efforts in the watershed. The study employed a multi-year before-and-after-control-impact (BACI) design in which physicochemical data were compared with numeric guidelines and biological data were compared with a variety of ecological metrics documented in

the literature. Among other conclusions, the study presented evidence that fish populations recover rapidly (i.e., within three generations) when water quality is improved, recovery rates vary for species having different sensitivities to various metals present in MIW, benthic macroinvertebrate communities recover at different rates than fish, and concentrations of cobalt (Co) and Cu (the dominant toxic metals in that system) in cobble and the water column played a dynamic role in ecological recovery in those MIW. Additionally, the study identified streambed cobble as an enduring sink of exchangeable metals that could be released back into the water column, thereby delaying ecological recovery.

Although these and other studies have begun to examine the biological and chemical responses of some MIW to remediation, ecotoxicological responses to AMD treatment remain largely unknown. To better predict the recovery patterns of aquatic organisms in MIW during treatment, a fundamental understanding of the bioavailability of toxicologically relevant chemical species throughout the remediation process will be needed.

1.4 Reverse isotopic labeling as a measure of copper bioavailability

Elevated Cu concentrations are a common feature of MIW in areas impacted by hard rock mining. Although Cu is an essential micronutrient in humans³⁰ and in all aquatic organisms,^{31,32} including the freshwater snail *Lymnaea stagnalis*,³³ it can cause toxicity in aquatic and terrestrial organisms at elevated concentrations.^{34,35} Determinations of bioavailability, herein defined as the proportion of a contaminant taken up from environmental media by an organism, can be crucial for understanding contaminant toxicity in environmental materials. Tracers have long been used in environmental toxicology to track trace metals and nutrients through organismal absorption, excretion, and transport pathways, allowing for determinations of contaminant bioavailability.³⁶⁻³⁸ Currently, the most commonly used types of tracers are

radioactive isotopes and stable isotopes.^{39,40} Although both have advantages and disadvantages, the use of radioactive isotopes can pose several challenges including waste management, safety hazards, and extensive permitting. Additionally, some elements, including Cu, lack radioisotopes suitable for research purposes due to short half-lives and preparatory challenges.⁴¹

Radioisotopes and stable isotopes have traditionally been used in environmental toxicology to label environmental media. In the case of metals, however, chemical speciation and location in particles can be highly variable,⁴¹ making the labeling of each geochemical phase in an environmental sample extremely difficult. In 2013, Croteau et al.⁴¹ published a method for the study of Cu bioavailability in natural particles that circumvented these issues by labeling the experimental organism instead of its food. In their procedure, the freshwater snail *L. stagnalis* is grown for several weeks in aquaria spiked with ⁶⁵Cu, the less naturally abundant stable isotope of Cu. This growth period results in the reversal of the isotopic signature of snail tissues from the natural abundance of ~70% ⁶³Cu and ~30% ⁶⁵Cu (i.e., ⁶⁵Cu:⁶³Cu ratio ≈ 0.4) to ~20% ⁶³Cu and ~80% ⁶⁵Cu (i.e., ⁶⁵Cu:⁶³Cu ratio ≈ 4.0). Snails are then fed a mixture of benthic algae and Cu-containing particles having natural isotopic abundance. Changes in snail tissue ⁶³Cu concentrations are then tracked throughout the exposure period (Figure 1.1).

Natural particles used by Croteau et al.⁴¹ in their original publication of the method were cobble coatings from the mining-influenced Animas River in Colorado. That study established the method's applicability to mining-influenced systems. Since then, the method has been applied to silver nanoparticles,⁴² to Cu sorbed to hydrous iron oxide,⁴³ and to Cu in loose, armored, and mixed cobble coatings from a mining-influenced system.⁴⁴ Croteau and authors⁴⁵

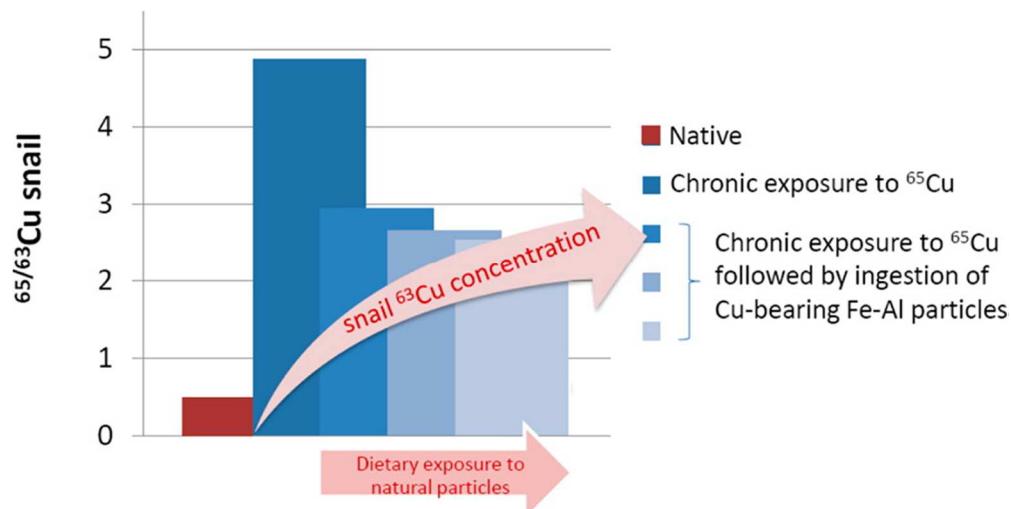


Figure 1.1 Illustrative graph showing $^{65}/^{63}\text{Cu}$ ratios in snail tissues, beginning with reversal (chronic exposure to ^{65}Cu) followed by a decrease with exposure to increasing amounts of Cu-containing natural particles⁴¹

had also previously used a similar method to determine bioavailability of zinc oxide nanoparticles. However, I am unaware of any uses of this reverse-labeling, stable-isotope method to track potential changes in contaminant bioavailability during a period of MIW remediation.

1.5 History of mining and remediation on North Fork Clear Creek

The study site for this research is the North Fork of Clear Creek (NFCC) in Black Hawk, Gilpin County, Colorado. NFCC is a southeast-flowing tributary of Clear Creek, which flows east from its headwaters in the Rocky Mountains of Colorado to its confluence with the South Platte River just north of Denver, Colorado. The creek was heavily influenced by hardrock mining activities beginning in the 1850s, at which point NFCC became contaminated with AMD.

The first known discovery of gold in the Clear Creek watershed occurred in January of 1859 by the prospector George Jackson, who had previously sought gold in California.⁴⁶ When news of this discovery spread, John H. Gregory, a prospector then working in Wyoming, made his way south to Colorado. Gregory first detected substantial amounts of gold in the waters of Clear Creek, the source of which he traced to a gulch in the mountains around Black Hawk and

the adjacent town of Central City. In May 1859, Gregory and a team of prospectors found the first recorded lode in Colorado history in what would come to be known as Gregory Diggings (Figure 1.2).⁴⁶

News of gold in Black Hawk and Central City drew thousands of prospectors from across the United States, and as veins were mined more intensively, the need for mills and smelters grew. Though smelters could be operated in the plains, mills were constructed on the banks of NFCC and Clear Creek so that operators could employ free water power. These construction

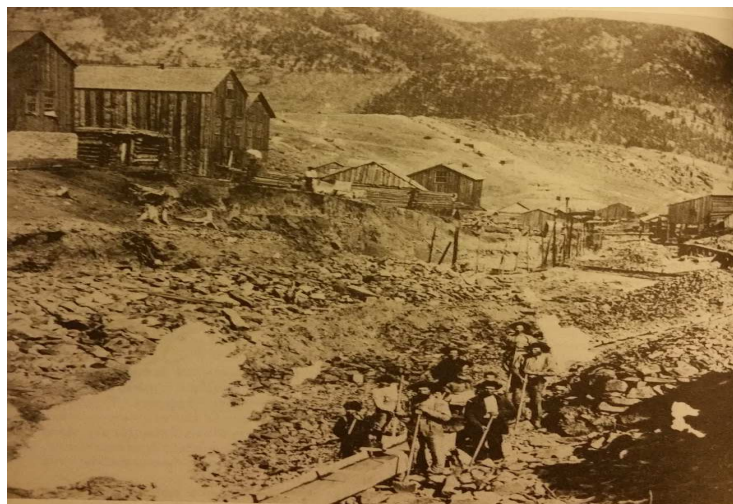


Figure 1.2 Photograph of the Gregory Diggings in Central City, CO, 1859 or 1860⁴⁶

operations brought mining processes directly to the streambanks, thereby exacerbating AMD generation along NFCC (Figure 1.3).

With the introduction of milling and smelting into gold and silver mining processes, the hardrock mining industry in Black Hawk and Central City boomed until the 1890s. By 1893, silver, which had brought a second economic boom to the state of Colorado, drastically declined in value, signaling a shift in the economics of the statewide hardrock mining industry.⁴⁶ As mines were dug deeper into the mountains, an increasing need to pump water out of deep mining tunnels created an additional economic burden for mine operators to bear. In spite of these



Figure 1.3 Photograph of tailings piles and wasterock at the Gilpin-Eureka Mine, CO, 1819⁴⁶

growing pressures, mines in Black Hawk and Central City were able to survive due to improvements in smelting and the construction of the Argo Tunnel, which drained mines in the Clear Creek watershed. By the 1940s, the mining industry was again struggling due to the depletion of placer deposits in the region. On January 19, 1943, a major flood in the Argo Tunnel killed several miners, leading to the permanent closure of the tunnel.⁴⁷ Despite a brief resurgence in small-scale mining in the 1970s, the regional hard rock mining industry never recovered, and the many claims dotting the western Colorado landscape were abandoned.

In September 1983, the Central City Clear Creek Watershed was officially named a Superfund site.⁴⁵ Following this designation, cleanup efforts began as a joint effort among the Colorado Department of Public Health and Environment (CDPHE), the United States Environmental Protection Agency (USEPA), and the communities in Central City and Black Hawk.

One of the first stages of cleanup involved the stabilization of two major tailings piles in 1988, followed by the construction of retaining walls and runoff control for two additional piles in 1999.⁴⁸ The Argo Tunnel Water Treatment Plant was constructed in Idaho Springs (on the other side of the geographic divide between NFCC and the main stem of Clear Creek) in 1998

during a subsequent remediation stage, and began treating AMD from the Argo Tunnel, Big Five Tunnel, and Virginia Canyon that were impacting the main stem of Clear Creek.⁴⁸ The plant is a lime-based active treatment, high-density sludge (HDS) facility that must be continuously operated to remove metals from the Argo Tunnel water. The final stage of remediation began in 2010 with the removal of five major and several secondary tailings piles along Virginia Canyon Road in the summer of 2010. Piles were excavated and consolidated at the Rio Grande waste area in Monte Vista, Colorado.⁴⁸ Finally, remediation efforts for the Central City Clear Creek Watershed culminated in March of 2017 with the completion of the North Fork Clear Creek Water Treatment Plant. Similar to the Argo Tunnel Treatment Plant, the North Fork Clear Creek Treatment Plant is a lime-based active treatment HDS facility that is treating two major point sources along NFCC.⁴⁹ The first of these sources, Gregory Incline, previously entered NFCC ~1.8 km upstream of the treatment plant, while the second, National Tunnel, entered the stream ~0.8 km upstream of the plant. Treatment of AMD from Gregory Incline and National Tunnel began in late March and mid-July of 2017, respectively.

1.6 Thesis objectives

The primary goal of this thesis is to begin to close the information gap in the literature about the responses of MIW to treatment. This research tests the hypothesis that Cu bioavailability in metal-oxyhydroxide cobble coatings differs between pre- and post-remediation samples. Two distinct types of cobble coatings (loose floc and armored coatings) are present in most AMD-contaminated streams. Armored coatings were selected as the experimental material in this research given that loose floc is scoured from cobble relatively quickly and is therefore less ecologically relevant to the long-term recovery of these systems. This idea was supported by visual monitoring observations that the loose floc in NFCC had been mostly or entirely removed

from cobble by August 2017 (i.e., within one spring runoff cycle), while some armored metal-oxyhydroxide coatings still remained.

Additionally, this research applied an established method of determining metal bioavailability in natural systems to a temporally changing stream ecosystem undergoing AMD remediation, while also testing the limits of the method with regards to organism size (mass). In this work, the methods of Croteau et al.⁴¹ were altered slightly to explore if, logistically, two different types of material could be investigated during the same experiment. This was deemed necessary to avoid batch-to-batch variability that could potentially arise while culturing and reverse-labeling snails, and thus could confound interpretation of the results. Additionally, organisms used in all experiments for this research were considerably smaller than those in the original method of Croteau et al.⁴¹ In the future, this information about sources of variability arising from the use of small (0.5-5 mg dry weight) organisms were used to adapt the methods of Croteau et al.⁴¹ for use with species that are smaller than pond snails, but are more ecologically relevant to high-gradient, montane streams.

1.7 References

- (1) Watkins, T. H. Hard rock legacy. *National Geographic*, Mar. 2000, 197 (3).
- (2) Mittal, A. K. *Abandoned mines: information on the number of hardrock mines, cost of cleanup, and value of financial assurances*; GAO-11-834T; United States Government Accountability Office: Washington, 2011; www.gao.gov/assets/130/126667.pdf.
- (3) Lyon, J. S. *Burden of guilt: the legacy of environmental damage from abandoned mines, and what America should do about it*; Mineral Policy Center: Washington, DC, 1993.
- (4) Concentration of abandoned mines, 2016. AbandonedMines.gov Home Page. <http://www.abandonedmines.gov> (Accessed Jan 6, 2018).
- (5) Jabeen, G.; Javed, M. Evaluation of arsenic toxicity to biota in river Ravi (Pakistan) aquatic ecosystem. *Int. J. Agric. Biol.* **2011**, 13 (6), 929-934.

- (6) Qu, R. -J.; Wang, X. -H.; Feng, M. -B.; Li, Y.; Liu, H. -X.; Wang, L. -S.; Wang, Z. -Y. The toxicity of cadmium to three aquatic organisms (*Photobacterium phosphoreum*, *Daphnia magna* and *Carassius auratus*) under different pH levels, *Ecotoxicol. Environ. Saf.* **2013**, 95, 83-90; DOI 10.1016/j.ecoenv.2013.05.020
- (7) Naddy, R. B.; Stubblefield, W. A.; May, J. R.; Tucker, S. A.; Hockett, J. R. The effect of calcium and magnesium ratios on the toxicity of copper to five aquatic species in freshwater, *Environ. Toxicol. Chem.* **2002**. 21 (2), 347-352; DOI 10.1002/etc.5620210217.
- (8) Custer, K. W.; Hammerschmidt, C. R.; Burton, G. A. Nickel toxicity to benthic organisms: the role of dissolved organic carbon, suspended solids, and route of exposure, *Environ. Pollut.*, **2016**. 208, 309-317; DOI 10.1016/j.envpol.2015.09.045.
- (9) Brix, K. V.; Esbaugh, A. J.; Munley, K. M.; Grosell, M. Investigations into the mechanism of lead toxicity to the freshwater pulmonate snail, *Lymnaea stagnalis*, *Aquat. Toxicol.*, **2012**. 106-107, 147-156; DOI 10.1016/j.aquatox.2011.11.007.
- (10) Khangarot, B.; Rajbanshi, V. Experimental studies on toxicity of zinc to a freshwater teleost, *Rasbora daniconius* (Hamilton), *Hydrobiologia*, **1979**. 65 (2), 141-144; DOI 10.1007/BF00017419.
- (11) Silverman M. P.; Ehrlich, H. L. Microbial formation and degradation of minerals, *Adv. Appl. Microbiol.*, **1964**. 6, 153-206; DOI 10.1016/S0065-2164(08)70626-9.
- (12) *Liquid assets 2000: America's water resources at a turning point*; Technical Report EPA-840-B-00-001; United States Environmental Protection Agency: Washington, DC, 2000; <https://nepis.epa.gov/Exe/ZyPDF.cgi/20004GRW.PDF?Dockey=20004GRW.PDF>.
- (13) Nordstrom, D. K. Mine waters: acidic to circumneutral. *Elements*, 2011, 7 (6), 393-398; DOI 10.2113/gselements.7.6.393.
- (14) Moran, R. E. and Wentz, D. A. *Effects of metal-mine drainage on water quality in selected areas of Colorado*; U.S. Geological Survey: Denver, CO, Circ. no. 25, 1974.
- (15) Kimball, B. A.; Broshears, R. E.; McKnight, D. M.; Bencala, K. E. Effects of instream pH modification on transport of sulfide-oxidation products. In *Environmental geochemistry of sulfide oxidation*; Alpers, C. N., Blowes, D. W., Eds., ACS Symposium Series 550; American Chemical Society: Washington, D.C., **1994**; pp. 224-243.
- (16) Broshears, R. E.; McKnight, D. M.; Runkel, R. L.; Kimball, B. A.; Bencala, K. E. Reactive solute transport in an acidic stream – experimental pH increase and simulation of controls on pH, aluminum, and iron, *Environ. Sci. Technol.* **1996**. 30 (10), 3016-3024; DOI 10.1021/es960055u.
- (17) Moncur, M. C. Acid mine drainage: past, present...future?. Univ. Waterloo. <http://uwaterloo.ca> (Accessed Mar 6, 2018).

- (18) Nordstrom, D. K.; Alpers, C. N. Geochemistry of acid mine waters. In *Reviews in Economic Geology, Vol. 6A: The Environmental Geochemistry of Mineral Deposits – Part A, Processes, Techniques, and Health Issues*; Plumlee G. S., Logsdon, M. J., Eds.; Society of Economic Geologists, Inc.: Littleton, CO 1999; pp. 131-160.
- (19) Zhu, M.; Legg, B.; Zhang, H.; Gilbert, B.; Ren, Y.; Banfield, J. F.; Waychunas, G. A.; Early stage formation of iron oxyhydroxides during neutralization of simulated acid mine drainage solutions. *Environ. Sci. Technol.* **2012**, 46, 8140-8147; DOI 10.1021/es301268g.
- (20) *Integrated investigations of environmental effects of historical mining in the Animas River Watershed, San Juan County, Colorado*; U.S. Geological Survey: Reston, VA, **2007**.
- (21) Rose, J.; Manceau, A.; Bottero, J. –Y.; Masion, A.; Garcia, F. Nucleation and growth mechanisms of Fe oxyhydroxide in the presence of PO₄ ions. 1. Fe K-Edge EXAFS study. *Langmuir* **1996**, 12 (26), 6701-6707.
- (22) Masion, A.; Doelsch, E.; Rose, J.; Moustier, S.; Bottero, J. Y.; Bertsch, P. M. Speciation and crystal Chemistry of iron(III) chloride hydrolyzed in the presence of SiO₄ ligands. 3. Semilocal scale structure of the aggregates. *Langmuir* **2001**, 17 (16), 4753-4757.
- (23) Webster, J. G.; Swedlund, P. J.; Webster, K. S. Trace metal adsorption onto an acid mine drainage iron(III) oxy hydroxy sulfate. *Environ. Sci. Technol.* **1998**, 32 (10), 1361-1368; DOI 10.1021/ew9704390.
- (24) Johnson, D. B.; Hallberg, K. B. Acid mine drainage remediation options: a review. *Sci. Total Environ.* **2005**, 338 (1-2), 3-14; DOI 10.1016/j.scitotenv.2004.09.002.
- (25) Kruse, N. A.; DeRose, L.; Korenowsky, R.; Bowman, J. R.; Lopez, D.; Johnson, K.; Rankin, E. The roles of remediation, natural alkalinity sources and physical stream parameters in stream recovery. *J. Environ. Manage.* **2013**, 128, 1000-1011; DOI 10.1016/j.jenvman.2013.06.040.
- (26) Williamson, J. L. Development and application of field methods for determination of the extent of acid mine drainage contamination and geochemical characteristics of stream cobble recovery. Ph.D. Dissertation, Colorado School of Mines, Golden, CO, 2016.
- (27) Ross, R. M.; Long, E. S.; Dropkin, D. S. Response of macroinvertebrate communities to remediation-simulating conditions in Pennsylvania streams influenced by acid mine drainage. *Environ. Monit. Assess.* **2008**, 145, 323-338; DOI 10.1007/s10661-007-0042-3.
- (28) Clements, W. H.; Vieira, N. K.; Church, S. E. Quantifying restoration success and recovery in a metal-polluted stream: a 17-year assessment of physicochemical and biological responses. *J. Appl. Ecol.* **2010**, 47 (4), 899-910; DOI 10.1111/j.1365-2664.2010.01838.x.
- (29) Mebane, C. A.; Eakins, R. J.; Fraser, B. G.; Adams, W. J. Recovery of a mining-damaged stream ecosystem. *Elementa Sci. Anthropocene.* **2015**, 3; DOI 10.12952/journal.elementa.000042.

- (30) Olivares, M.; Uauy, R. Copper as an essential nutrient. *Am. J. Clin. Nutr.* **1996**, 63 (5), 791S-796S; DOI 10.1093/ajcn/63.5.791.
- (31) Lilly, T. T.; Immaculate, J. K.; Jamila, P. Macro and micronutrients of selected marine fishes in Tuticorin, South East coast of India. *Int. Food Res. J.* **2016**, 24 (1), 191-201.
- (32) Manahan, S. E.; Smith, M. J. Copper micronutrient requirement for algae. *Environ. Sci. Technol.* **1973**, 7 (9), 829-833; DOI 10.1021/es60081a013.
- (33) Sprong, N.; Brinkman, F. G.; Van Hoek, R. J.; Knook, D. L. Copper in *Lymnaea stagnalis* L.-II. effect on the kidney and body fluids. *Comp. Biochem. Physiol.* **1971**, 38A, 309-316; DOI 10.1016/0300-9629(71)90057-0.
- (34) Brewer, G. J. Risks of copper and iron toxicity during aging in humans. *Chem. Res. Toxicol.* **2010**, 23 (2), 319-326; DOI 10.1021/tx900338d.
- (35) Brix, K. V.; Esbaugh, A. J.; Grosell, M. The toxicity and physiological effects of copper on the freshwater pulmonate snail, *Lymnaea stagnalis*. *Comp. Biochem. Physiol.* **2011**, 154 (3), 261-267; DOI 10.1016/j.cbpc.2011.06.004.
- (36) Croteau, M. N.; Luoma, S. N.; Topping, B. R.; Lopez, C. B. Stable metal isotopes reveal copper accumulation and loss dynamics in the freshwater bivalve *Corbicula*. *Environ. Sci. Technol.* **2004**, 38, 5002-5009.
- (37) Wang, W. X.; Fisher, N. S. Assimilation efficiencies of chemical contaminants in aquatic invertebrates: a synthesis. *Environ. Toxicol. Chem.* **1997**, 18, 2034-2045.
- (38) Cain, D. J.; Croteau, M. N.; Fuller, C. C. Dietary bioavailability of Cu adsorbed to colloidal hydrous ferric oxide to freshwater benthic grazers. *Environ. Sci. Technol.* **2013**, 47 (6), 2869-2876; DOI 10.1021/es3044856.
- (39) Cornelis, R. Use of radiochemical methods as tools for speciation purposes in environmental and biological sciences. *Analyst.* **1992**, 117, 583-588.
- (40) Stürup, S.; Hansen, H. R.; Gammelgaard, B. Application of enriched stable isotopes as tracers in biological systems: a critical review. *Anal. Bioanal. Chem.* **2008**, 390, 541-554.
- (41) Croteau, M.-N.; Cain, D. J.; Fuller, C. C. Novel and nontraditional use of stable isotope tracers to study metal bioavailability from natural particles. *Environ. Sci. Technol.* **2013**, 47, 3424-3431; DOI 10.1021/es4000162f.
- (42) Yu, S. J.; Yin, Y. G.; Zhou, X. X.; Dong, L. J.; Liu, J. F. Transformation kinetics of silver nanoparticles and silver ions in aquatic environments revealed by double stable isotope labeling. *Environ. Sci. Nano.* **2016**, 3 (4), 883-893; DOI 10.1039/c6en00104a.

- (43) Cain, D. J.; Croteau, M. N.; Fuller, C. C.; Ringwood, A. H. Dietary uptake of Cu sorbed to hydrous iron oxide is linked to cellular toxicity and feeding inhibition in a benthic grazer. *Environ. Sci. Technol.* **2016**, 50 (3), 1552-1560; DOI 10.1021/acs.est.5b04755.
- (44) Traudt, E. M. Evaluation of toxicity and bioavailability of metal mixtures to two freshwater invertebrates. Ph.D. Dissertation, Colorado School of Mines, Golden, CO, 2016.
- (45) Croteau, M. N.; Dybowska, A. D.; Luoma, S. N.; Valsami-Jones, E. A novel approach reveals that zinc oxide nanoparticles are bioavailable and toxic after dietary exposures. *Nanotox.* **2011**, 5 (1), 79-900; DOI 10.3109/17435390.2010.501914.
- (46) Cox, T. *Inside the Mountains: A History of Mining Around Central City, Colorado*; Pruett Publishing Company: Boulder, CO, 1989.
- (47) Jessen, K. The Deadly End to the Argo Tunnel. *The Loveland Reporter-Herald*, Sep. 18, 2011.
- (48) *Update Fact Sheet*; Colorado Department of Public Health and Environment, Denver, CO, 2015.
- (49) *Grand Opening Fact Sheet: Central City/Clear Creek Superfund Site*; Colorado Department of Public Health and Environment, Denver, CO, 2017.

CHAPTER 2

DIETBORNE BIOAVAILABILITY OF COPPER IN ACID MINE DRAINAGE-RELATED PARTICLES TO FRESHWATER SNAILS (*LYMNAEA STAGNALIS*), AND THE IMPORTANCE OF ORGANISM SIZE IN A REVERSE-LABELING STABLE-ISOTOPE METHOD

2.1 Abstract

Although the detrimental environmental impacts of acid mine drainage (AMD) have been extensively researched, little is known about the temporal responses of mining-influenced systems to remediation efforts. To address this information gap, we examined the bioavailability of copper (Cu) from metal-oxyhydroxide cobble coatings collected from the North Fork of Clear Creek (NFCC) in Black Hawk, Gilpin County, Colorado. For more than a century, NFCC was contaminated with AMD, until the completion of a high-density-sludge lime treatment plant in March 2017. Using an innovative reverse-labeling stable-isotope method developed by U.S. Geological Survey researchers, we calculated Cu assimilation efficiency (AE) in freshwater snails (*Lymnaea stagnalis*) that were fed cobble-coating particles collected from NFCC before and several months after remediation of the AMD.

Although Cu bioavailability did not differ significantly between pre- and post-remediation metal-oxyhydroxide particles (~34% AE), high among-replicate variability and small number of organisms resulted in low statistical power to infer significant differences. Our use of small organisms (~0.5-5 mg dry tissue weight) in the experiments may have contributed to the relatively high variability, especially related to estimation of differences in tissue Cu concentrations between exposed and background snails, which is required to calculate AE. A novel finding is that background copper concentrations decreased with increasing size and followed the relationship: $[^{63}\text{Cu}]_{\text{snail}} = 70.088 \times M_{\text{snail}}^{-0.628}$. These size constraints may have

important implications for the planned adaptation of this method to smaller benthic organisms that are more ecologically relevant in high-gradient, montane streams (e.g., the midge *Chironomus dilutus*).

2.2 Introduction

Mining influenced waters (MIW) are an extremely complex and widespread environmental issue impacting a large number of mines across the United States. Due to poor documentation of mining activities during the United States' hardrock mining boom in the 1800s, current estimates place the total number of American abandoned mines between 160,000 and 500,000.^{1,2} Although the detrimental environmental impacts of MIW and the biogeochemical mechanisms governing its generation have been well-documented in the literature, few studies have examined the real-time responses of MIW to remediation efforts. Clements et al.³ presented one of the first major efforts to close this information gap in 2010 with the publication of one of the most comprehensive studies of physicochemical and biological data for MIW to date. The study comprised 17 years of seasonal and annual measurements of water quality, metal concentrations in cobble, macroinvertebrate communities, and brown trout populations before and after several stages of restoration and remediation on the Arkansas River near Leadville, Colorado. Results of the study revealed that remediation success varied seasonally, spatially, and among response variables, as well as that the determination of whether or not MIW have recovered following treatment is further complicated by potential differences in recovery rates of cobble and the water column.

Although that and other studies have made great strides in examining chemical and biological responses to MIW remediation, little is known about changes in toxicological parameters (e.g., bioavailability of metals in streambed cobble coatings) that may occur in MIW

during treatment. To address this knowledge gap, we compared copper (Cu) bioavailability in armored metal-oxyhydroxide cobble coatings from the North Fork of Clear Creek (NFCC) in Black Hawk, Colorado to discern whether or not the Cu bioavailability in armored cobble coatings changes following the removal of metal inputs from the water column. For the purposes of this research, Cu bioavailability is herein defined as the proportion of the total Cu to which organisms are exposed, that is accumulated in their soft tissue over a defined exposure period.

NFCC was heavily influenced by gold and silver mining activities between the 1850s and the 1970s, beginning with the 1859 prospecting of the Gregory Diggings and ending with the drawn out collapse of the hard rock mining industry in the Clear Creek watershed beginning with the 1943 flooding of the Argo Tunnel.⁴ A portion of the watershed, including Black Hawk, was designated a Superfund site in 1983, at which point cleanup efforts were commenced by the Colorado Department of Public Health and Environment (CDPHE), the United States Environmental Protection Agency (USEPA), and the local communities of Black Hawk and Central City.⁵ Remediation efforts culminated in the construction of a high-density sludge (HDS) lime treatment plant on NFCC that became operational in May 2017.⁶

To assess Cu bioavailability in cobble coatings, we selected a reverse-labeling, stable isotope method devised by Croteau et al.⁷ in which Cu assimilation efficiency (AE) is calculated in freshwater snails (*Lymnaea stagnalis*). Copper is a micronutrient for *L. stagnalis*,⁸ and is thus present at measurable background concentrations in the test organisms. *L. stagnalis* also regulate Cu very effectively.⁸ The combined effects of these two factors make the detection of changes to tissue Cu concentrations in the organisms, resulting from dietary exposure to Cu-contaminated sediments, difficult at sublethal exposure concentrations. This detection issue is meant to be circumvented in the reverse-isotope labeling method by loading test organisms with the less

naturally abundant ^{65}Cu isotope for between 4 and 6 weeks before experimentation, resulting in the effective reversal of Cu isotopic signatures in the snails. During the experiment, changes in the ^{65}Cu : ^{63}Cu isotopic signature in the snails are tracked as snails ingest bioavailable Cu having the natural (~ 0.44) ^{65}Cu : ^{63}Cu isotopic signature.

While *L. stagnalis* are ecologically relevant to limnic ecosystems, they are not representative of the types of species found in high-gradient, montane streams. Moreover, most invertebrate species that are ecologically relevant to these types of systems are smaller than *L. stagnalis*. To begin working towards adapting this method to species more ecologically relevant to the types of ecosystems impacted by MIW in much of the western United States, we selected snails spanning a range of small weights (~ 0.5 -5 mg dry tissue weight) in an attempt to test the limits of this method with regards to organism size. Our results may prove helpful for determinations of organism-size constraints for methods of determining contaminant bioavailability.

2.3 Methods

2.3.1 Collection, preparation, and characterization of armored metal oxyhydroxide cobble coatings from North Fork Clear Creek

2.3.1.1 Cobble collection and preparation of cobble coatings

Cobble for bioavailability experiments was collected from the stream bed in February and August 2017. The February sampling occurred before any diversion or treatment of the AMD point sources. The August sampling date was 4 mo post-treatment of the Gregory Incline point source and 1 mo post-treatment of the National Tunnel point source. Samples were collected at a site 0.4 km downstream of the treatment plant effluent discharge point, named Railless Below Plant (RBP) (Figure 2.1). On each sampling date, 30 subsamples of rocks and cobble were randomly selected from a 50-m riffle zone at the RBP site and placed in a polyethylene sealable

bag (Ziploc®). Bags containing samples were stored in a refrigerator overnight at 10°C until they could be fully processed 1 d after sample collection. To isolate the armored cobble coatings, loose metal-oxyhydroxide cobble coatings (floc) were first removed from cobble. The loose floc was removed by gently rubbing the cobble for ~2 min from outside the bag after a known volume of deionized (DI) water had been added. In a pilot experiment, we determined that insignificant amounts of additional loose floc were removed when cobbles were rubbed for > 2 min. After the removal of loose floc, cobbles were placed in a rock tumbler with a known volume of DI water. The rock-water mixture was then slowly rotated for 2 h to remove the armored coating. In the same pilot experiment, the cobble began to be pulverized and insubstantial additional amounts of armored coating were removed when

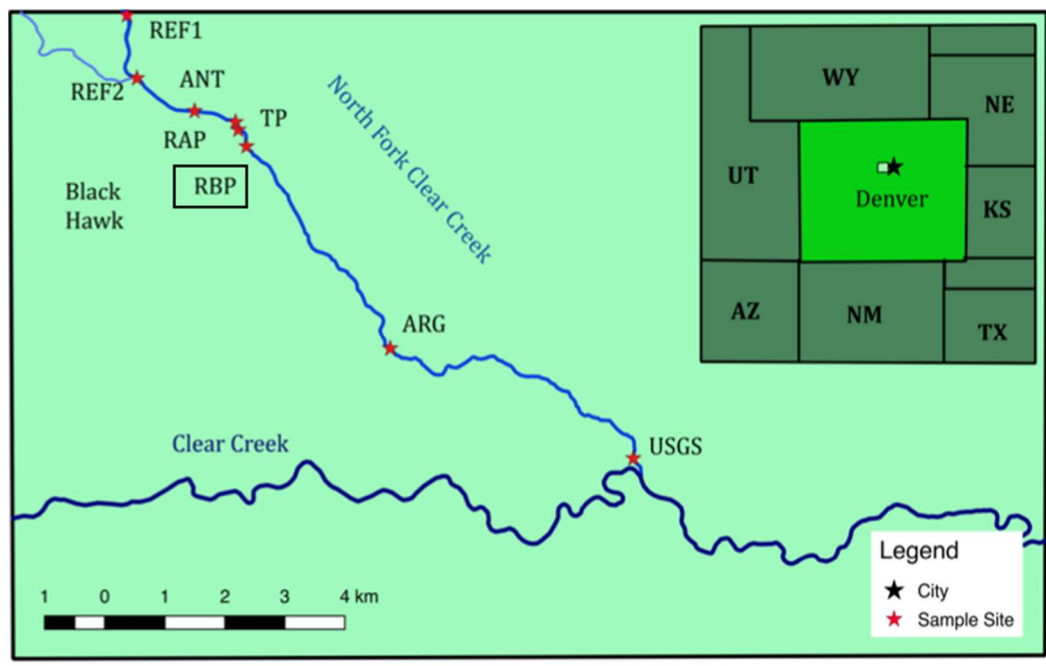


Figure 2.1 Map of the North Fork of Clear Creek, Gilpin County, Colorado, showing stream sites. Treated acid mine drainage water enters the stream at the North Fork Clear Creek Water Treatment Plant (TP); cobble was collected at RBP (Railless Below Plant) is where cobble were hand-picked.

tumbling exceeded 2 h. The resulting North Fork particle suspensions (NFPS) of armored metal-oxyhydroxide coatings were poured into 1-L high-density polyethylene (HDPE) bottles (Nalgene™). Cobbles were rinsed with 50 ml of DI water, and the rinse was added to the rest of the NFPS. NFPS was then stored at -40°C until its use in characterization and bioavailability experiments.

Forty-eight h before the bioavailability experiments could be performed, the Cu content of the NFPS needed to be determined. NFPS solutions from each sample date were removed from the freezer and allowed to thaw at room temperature (25°C) for 24 h. After thawing, NFPS solutions were digested (Section 2.3.1.4) and then analyzed for elemental composition (Section 2.4.1.3).

A portion of each NFPS was diluted with DI water to achieve total Cu concentrations of ~1000 µg L⁻¹ for use in Cu bioavailability experiments. Remaining NFPS solutions were set aside to be further characterized. NFPS Cu concentrations were determined using a PerkinElmer Optima 7300 inductively coupled plasma-atomic emission spectrometer (ICP-AES).

In addition to cobble collection, stream pH, conductivity, ferrous iron, and temperature were measured in the field. Water samples were also collected, filtered (0.45-µm Millipore syringe filters), and acidified to 5% with 16 N HNO₃ (Fischer Scientific, trace metal grade) for analysis of dissolved cations. Unfiltered water samples were also collected and acidified to 5% with 16 N HNO₃ (Fischer Scientific, trace metal grade) for analysis of total cations. Filtered but non-acidified samples were collected for dissolved anions. Filtered and unfiltered samples were collected and acidified to 2% with 12 N HCl (Fischer Scientific, trace metal grade) for analysis of dissolved and total organic carbon, respectively. Total and dissolved cation concentrations were analyzed using a PerkinElmer Optima 7300 inductively coupled plasma-atomic emission

spectrometer (ICP-AES), dissolved anion concentrations were analyzed using a Dionex DC 80 ion chromatograph (IC), and total organic carbon (TOC) and dissolved organic carbon (DOC) concentrations were analyzed using a Shimadzu TOC-L analyzer.

2.3.1.2 X-ray diffraction

Cobble coatings were characterized for mineralogy using x-ray diffraction (XRD). Oriented aggregate mount XRD samples were prepared from suspensions of NFCC armored metal-oxyhydroxide particles removed from cobble collected in February 2017 and August 2017 for 2 grain size fractions: <2 mm and <2 μm . The <2-mm samples were prepared by wet-sieving each suspension through a 2-mm sieve, and then vacuum filtering the resulting mineral suspensions onto 0.45- μm nominal pore opening cellulose filters (Millipore). Filters were then wrapped around a plastic cylinder, and quickly rolled across a glass slide to transfer mineral films onto the sample mounts. The <2- μm clay size fraction samples were prepared by first centrifuging 50 ml of NFPS mineral suspensions for 60 s at 1000 rpm (as determined from theoretical Stokes Law Calculations¹⁴), and then filtered and transferred to glass slides as was done for the <2-mm grain size fraction samples. Sample scans were performed using a Scintag XDS 2000 x-ray diffractometer that employs Cu-K α radiation. All mineral scans were continuous, analyzing samples from 4-50° 2 theta with a step size of 0.2° and a counting time of 2 s. XRD data analyses were performed using Scintag DMS-NT software to identify diagnostic mineral peaks.

2.3.1.3 Electron microscopy: VP-SEM and TIMA3

Cobble coatings were also characterized by automated variable pressure-scanning electron microscopy (VP-SEM). Samples were prepared by filtering 0.5 ml of NFPS from each sampling date onto 0.2- μm polycarbonate filters (Millipore). Filters were carbon coated and

mounted on glass slides using carbon tape. NFPS samples were loaded into a TESCAN-VEGA-3 Model LMU VP-SEM platform, and analyzed using the control program TIMA3.

Four energy dispersive X-ray (EDX) spectrometers acquired spectra from each particle with a beam stepping interval (i.e., spacing between acquisition points) of 30 μm , an accelerating voltage of 25 keV, and a beam intensity of 14. Interactions between the beam and the sample were modeled through Monte Carlo simulation. The TIMA3 software identified mineral phases by comparing acquired EDX spectra with known spectra stored in the software database. The software does not, however, distinguish between crystalline mineral phases and amorphous material of the same elemental composition. In addition to providing mineralogic characterization, TIMA3 was used to generate element maps of Fe and Si distribution in both samples. Characteristic x-ray emission lines are acquired by the VP-SEM and matched to emission lines of elements by the TIMA3 software. Intensities (counts per second; cps) of peaks detected by the software are used as a qualitative measure of relative element concentrations across a sample, and mapped using a grayscale, with brighter spots indicating higher element concentrations and darker spots indicating lower element concentrations.

2.3.1.4 Analyses of armored cobble coating copper content

For analyses of cobble-coating Cu content, 2-ml samples of NFPS prepared from February 2017 and August 2017 cobble were pipetted into pre-weighed 15-ml Falcon tubes and allowed to dry in an oven at 40°C for several days. Once fully dried, all samples were re-weighed and digested using USEPA Method 3051a (Microwave Assisted Acid Digestion of Cobble, Sludges, Soils, and Oils).¹⁵ Digested samples were diluted to 5% acidity and analyzed by ICP-AES. Sample Cu concentrations were then used to calculate total Cu concentrations in the NFPS.

2.3.2 Copper bioavailability experiments

2.3.2.1 Materials preparation

Before starting the experiments, all glassware, tweezers, dissection trays, Teflon, feeding cups, and depuration chambers were acid washed to prevent metal contamination. Feeding cups and depuration chambers were soaked for 24 h in 10% hydrochloric acid, while all other materials were soaked in 15% nitric acid. All materials were then rinsed several times with Milli-Q water.

2.3.2.2 Test organisms

Freshwater snails (*Lymnaea stagnalis*) have been used extensively in other bioavailability studies,^{9,10} and were used in all experiments. The snails were bred and raised in the laboratory at room temperature (15-20°C) in aquaria containing ~10 L of USEPA Moderately Hard Reconstituted Water (MHRW).¹¹ Snails were fed a diet of lettuce *ad libitum* and grown for ~3 mo before each experiment. The average dry weight per test organism at the start of the bioavailability experiments was 1.7 ± 1.3 mg (\pm SD).

2.3.2.3 Isotopic reversal and dietborne exposures

Copper bioavailability to *L. stagnalis* exposed to armored cobble coatings was examined using an adaptation of the procedure described by Croteau et al.⁷ Copper bioavailability in armored cobble coatings collected from NFCC before treatment (February 2017) was compared to Cu bioavailability in armored cobble coatings collected from NFCC after treatment (August 2017). For ~4 weeks before the dietborne exposure, snails were reared in an aquarium filled with ~10 L of MHRW, spiked with 2 ml of ⁶⁵Cu solution (~50 mg Cu/L, prepared from 99.4% Cu(NO₃)₂ [Trace Sciences]) and completely renewed weekly (i.e., MHRW was changed and new ⁶⁵Cu solution was added). The target Cu concentration in the aquarium was 10 µg L⁻¹ in the

MHRW. The goal of this process was to effectively reverse the snails' Cu isotopic ratios from the natural abundance (~30% ^{65}Cu :~70% ^{63}Cu) to ~75% ^{65}Cu :~25% ^{63}Cu . The snails were fed a diet of uncontaminated lettuce, but feeding was ceased 2 d before the experiment to allow the food to pass out of the snails' guts before starting the experimental period.

Ten d before the dietborne exposure, benthic diatoms (*Nitzschia palea*, University of Waterloo strain CPCC 160) having a natural Cu isotopic abundance were inoculated in S-diatom media⁷ and grown axenically to be used as a food source during the exposures. After 10 d of growth, diatoms were vacuum filtered onto 1.2- μm Isopore membrane filters (Millipore) and then rinsed into a large acid-washed beaker using USEPA Soft Water.¹¹ Sixty ml of the concentrated diatom solution was mixed with sufficient volumes of the diluted NFPS from each respective sampling date to reach a target concentration in the feeding mat of ~600 $\mu\text{g Cu g}_{\text{mat}}^{-1}$ (g metal-oxyhydroxide coating + g diatom) (Table 2.1). This target Cu concentration is calculated assuming no significant amount of Cu is contributed by the diatoms. This assumption was not correct for this experiment and will be discussed in the Results section of this thesis. Additionally, a “control” feeding mat was prepared with 60 ml of diatom solution only. Final feeding mats were created by gently shaking diatom-NFPS mixtures for ~1 min, and then vacuum filtering the mixture onto 1.2- μm Isopore membrane (Millipore) filters. Duplicate feeding mats were prepared for all 3 materials (diatoms only, February 2017 Armor + diatoms, and August 2017 Armor + diatoms). A sliver of each feeding mat was excised and digested (Section 2.3.2.4) for analysis of Cu content using a Perkin Elmer NexION 300D inductively coupled plasma-mass spectrometer (ICP-MS). The remaining portions of the feeding mats were placed into separate acid-washed 150-ml polypropylene cups, which were then partially submerged in an aquarium filled with ~2 L of MHRW. Each of these polypropylene “feeding

chambers” had 2 holes cut in either side that were covered with fine (~250 µm) mesh to allow water to flow freely through the chamber. Fifty-four test organisms were removed from the breeding tank, divided such that 9 organisms were placed on each of the 6 feeding mats, and allowed to graze for 4 h. Additionally, 20 “background” snails were removed from the aquarium and immediately frozen at -40°C for future determination of the ⁶⁵Cu:⁶³Cu ratio of unexposed snails.

Table 2.1 Volumes and copper concentrations of North Fork Particle Suspensions (NFPS) used to create diatom-NFP feeding mats. Sixty ml of diatom suspension (15.85 mg diatom mass) was used to prepare each mat. The mass of diatom in 60 ml of diatom suspension was gravimetrically-determined 1 d before the exposure.

	Target [Cu] (µg Cu g _{mat} ⁻¹)	Nominal Mass Cu (µg)	[Cu] in NFPS (µg Cu L ⁻¹)	Vol NFPS (ml)
Diatoms only	0	0	-	0
2/17 Armor	600	9.5148	1000	9.51
8/17 Armor	600	9.5148	1039	9.16

After the feeding period, snails were removed from the feeding chambers and rinsed with MHRW. Each snail was then placed into a separate acid-washed 39-ml polypropylene chamber with a small amount of lettuce (~0.5 mg dry weight) to begin the depuration period. Each chamber had 2 holes cut into its sides that were secured with fine mesh to allow water to circulate freely through the chamber, preventing ammonia buildup. Additionally, the tops of the chambers were secured with fine mesh to allow the snails to surface during the depuration period. The depuration chambers were then partially submerged in an aquarium that contained ~30 L of MHRW and an aquarium filter for 48 h of depuration of the snails’ gut contents. At the end of the depuration period, the chambers were removed from the aquarium. Using an 8-ml

transfer pipet, water remaining in the depuration chambers and feces were harvested and transferred into 15-ml Falcon tubes. The size of the mesh prevented nearly all feces from escaping the depuration chambers during collection. Snails were then removed from the depuration chambers, rinsed with MHRW, and frozen (-10°C) for later dissection and soft-tissue analysis.

2.3.2.4 Sample preparation and chemical analyses

To determine the true Cu content of each feeding mat, the previously collected slivers were subdivided into five pieces, dried in an oven for 48 h at 40°C, weighed, and placed into 15-ml Falcon tubes. Falcon tubes of feces were also dried for 48 h at 40°C. Snails were removed from the freezer and dissected to separate their soft tissue from their shells. The soft tissue of each snail was placed onto an individual piece of acid-washed Teflon, and then into a petri dish to be dried for 48 h at 40°C. Teflon pieces were used to prevent snail soft tissue sticking to the petri dish during drying. Shells were discarded. Dried soft tissue was weighed and transferred into 15-ml Falcon tubes. Additionally, a sample of the batch of lettuce used during the depuration period was dried for 48 h at 40°C, weighed, and transferred into a 15-ml Falcon tube.

Two hundred µl of 16 N HNO₃ (Fischer Scientific, trace metal grade) was added to all Falcon tubes containing feeding mat samples, feces, snails, or lettuce. Samples were acid-digested for 5 to 6 d at 25°C, after which 80 µl of 30% H₂O₂ (Macron Fine Chemicals) was added to all samples. They were then digested for an additional 24 h at 25°C. Once fully digested, samples were diluted to a final volume of 4 ml with Milli-Q water.

All feeding mat, feces, snail, and lettuce samples were analyzed for ⁶³Cu and ⁶⁵Cu concentrations by a PerkinElmer NexION 300 inductively coupled plasma-mass spectrometer (ICP-MS). A solution containing 3 µg L⁻¹ germanium (Spex CertiPrep) in 2% HNO₃ (Fischer

Scientific, trace metal grade) was used as an internal standard for all measurements.

Additionally, two samples were prepared from NIST-2976 (mussel tissue) using the same digestion procedure as all other samples and were analyzed in all analytical runs. These two samples were within the range of certified total copper values ($4.02 \text{ mg kg}_{\text{tissue}}^{-1} \pm 0.33$) for all sample runs. During all analytical runs, a blank sample of 2% HNO_3 and a sample of NIST certified 1640a standard reference material solution¹² were run after every 10 samples and at the end of each analytical run. Standard results differing from the reported Cu values by more than $\pm 10\%$ were rejected, and all samples run after the rejected standards were rerun. The Cu detection limit for both isotopes during all runs was $0.037 \mu\text{g L}^{-1}$.

2.3.2.5 Data analysis

All calculations were performed using a modification of the procedure outlined by Croteau et al.⁷ In the Croteau et al.⁷ method, background tissue concentrations of ^{63}Cu ($\mu\text{g } ^{63}\text{Cu g}_{\text{snail}}^{-1}$) in each isotopically-reversed snail (defined as $[^{63}\text{Cu}]_{0,\text{snail}}$) are estimated using an experimentally-determined rate constant of Cu uptake from diatom-cobble coating feeding mats, and by accounting for losses of ^{63}Cu (using the efflux rate, k_e) that could have occurred during the feeding and depuration periods and gains in ^{63}Cu via uptake from lettuce during depuration. To calculate the rate of ^{63}Cu uptake from diatom-cobble coating mats, this method required that organisms be exposed to a range of Cu concentrations created by mixing varying volumes of a cobble coating suspension with diatoms. Due to logistical constraints, primarily organism rearing capacity, the Croteau et al.⁷ method is practically limited to the analysis of one type of material in each experiment.

Because we wanted to compare Cu bioavailability in NFCC armored metal-oxyhydroxide cobble coatings pre- and post-remediation simultaneously, we developed a second approach that

was a modification of the Croteau et al.⁷ method for determining Cu bioavailability. Rather than back-calculating $[^{63}\text{Cu}]_{0,\text{snail}}$, we measured the concentration of ^{63}Cu in the soft tissue of each of the 20 “background” snails. We initially used the average of these measured values (hereafter referred to as $[^{63}\text{Cu}]_{\text{b,snail}}$) to calculate the mass of ^{63}Cu (ng) accumulated by each snail during the exposure period. This was done by subtracting $[^{63}\text{Cu}]_{\text{b,snail}}$ from the concentration of ^{63}Cu measured in each snail’s soft tissue at the end of the exposure and depuration periods (defined as $[^{63}\text{Cu}]_{\text{snail}}$). In section 2.4.2 we describe a third approach in which we relate $[^{63}\text{Cu}]_{\text{b,snail}}$ to snail size and use a size-specific background ^{63}Cu concentration.

To distinguish between ^{63}Cu accumulated from diatoms and ^{63}Cu accumulated from metal-oxyhydroxide cobble coatings, we calculated $[^{63}\text{Cu}]$ accumulated from diatoms only ($[^{63}\text{Cu}]_{\text{d-b,snail}}$) by subtracting average $[^{63}\text{Cu}]_{\text{b,snail}}$ from the average tissue ^{63}Cu concentration measured in snails exposed to diatoms only ($[^{63}\text{Cu}]_{\text{d,snail}}$). ^{63}Cu accumulated from lettuce was calculated using biodynamic parameters for ^{63}Cu accumulated from lettuce (k_{lett}) and the rate constant of copper loss (k_{e}) determined by Croteau and coauthors.^{7,13} Finally, we calculated ^{63}Cu accumulated from metal-oxyhydroxide cobble coatings ($^{63}\text{Cu}_{\text{accumulated,NFPS}}$) by subtracting ^{63}Cu accumulated from lettuce and diatoms from $[^{63}\text{Cu}]_{\text{snail}}$ measured in organisms at the end of the experiment ($[^{63}\text{Cu}]_{\text{snail}}$) (Equation 2.1), where T_2 is the duration of the depuration period.

Definitions of parameters and values of constants used in bioavailability calculations are summarized in Table 2.2.

Table 2.2 Parameters used to calculate the total mass of ^{63}Cu (ng) accumulated from armored metal-oxyhydroxide cobble coatings in North Fork Particle Suspensions (NFPS) and Cu assimilation efficiency by *L. stagnalis* over a 4-h exposure period followed by a 2-d depuration period.

Parameter	Symbol	Units	Value
Mass of ^{63}Cu accumulated from NFPS only	$^{63}\text{Cu}_{\text{accumulated}}$	ng	-30.72 - 337.99 ^c

Table 2.2: Continued

Parameter	Symbol	Units	Value
Tissue ⁶³ Cu concentration measured in snails post-exposure	[⁶³ Cu] _{snail}	μg g ⁻¹	11.55 - 478.79 ^c
Background ⁶³ Cu concentration measured in snails	[⁶³ Cu] _{b,snail}	μg g ⁻¹	34.37 - 155.18 ^c
Tissue ⁶³ Cu concentration measured in snails exposed to diatoms minus background ⁶³ Cu	[⁶³ Cu] _{d-b,snail}	μg g ⁻¹	1.974
Rate constant of Cu uptake from lettuce ^a	k _{ulett}	g g ⁻¹ d ⁻¹	0.162
Concentration of ⁶³ Cu in lettuce	[⁶³ Cu] _{lett}	μg g ⁻¹	4.829
Rate constant of loss ^b	k _e	d ⁻¹	0.026
Duration of depuration period	T ₂	d	2
Mass of snail	M _{snail}	mg	0.2 - 4.56 ^c
Total mass of ⁶³ Cu in snail feces	⁶³ Cu _{feces}	ng	2.7 - 330.8 ^c

^a Determined by Croteau and Luoma¹³

^b Determined by Croteau et al.⁷

^c Range

$$\begin{aligned}
 {}^{63}\text{Cu}_{\text{accumulated,NFP}} &= ([{}^{63}\text{Cu}]_{\text{snail}} - ([{}^{63}\text{Cu}]_{\text{b,snail}} + [{}^{63}\text{Cu}]_{\text{d-b,snail}} \\
 &+ \frac{k_{\text{ulett}}[{}^{63}\text{Cu}]_{\text{lett}}}{k_e} (1 - \exp^{-k_e T_2})) \times M_{\text{snail}}
 \end{aligned} \tag{2.1}$$

Finally, assimilation efficiency (AE) was calculated as the percentage of ⁶³Cu ingested by each snail that was accumulated into the snail's soft tissue using Equation 2.2, where ⁶³Cu_{feces} is the total mass of ⁶³Cu measured in feces collected from each individual organism (ng). ⁶³Cu_{feces} values were determined by multiplying the concentration of ⁶³Cu measured in the feces digests ([⁶³Cu]_{feces}; as μg ⁶³Cu L⁻¹ of acid digest) by the final volume of each digested feces sample (4 ml).

$$\text{Assimilation Efficiency (\%)} = \frac{{}^{63}\text{Cu}_{\text{accumulated}}}{{}^{63}\text{Cu}_{\text{accumulated}} + {}^{63}\text{Cu}_{\text{feces}}} \times 100 \tag{2.2}$$

Significant differences in Cu bioavailability in February and August 2017 NFCC armored metal-oxyhydroxide cobble coatings were tested by single-factor ANOVA. Differences were considered to be significant at a type I error rate of $\alpha = 0.05$.

2.4 Results and discussion

2.4.1 Cobble coatings

2.4.1.1 X-ray diffraction

Based on XRD of the <2-mm and <2- μm size fraction of NFPS, the mineralogy of cobble coatings removed from NFCC cobble pre- and post-remediation was virtually identical. The <2-mm size fraction of material represented the material fed to the snails; the <2- μm size fraction was intended to contain only the cobble coatings, thus excluding other, larger detrital minerals that may have been broken away from cobbles during the rock tumbling process.

The <2-mm size fraction from both sampling dates contained a variety of detrital minerals that obscured amorphous metal-oxyhydroxide peaks (Figures 2.2 and 2.4). Detrital minerals dominating XRD patterns for the <2-mm size fraction included biotite, plagioclase feldspars, and quartz.

Analysis of the <2- μm size fraction of NFPS from February (Figure 2.3) and August 2017 (Figure 2.5) suggested that cobble coatings were a mixture of mostly amorphous, metal-oxyhydroxide materials. Sample diffraction patterns were featureless and did not resemble any known crystalline metal-oxide minerals. We concluded, therefore, that the cobble coatings were possibly a complex mixture of amorphous, metal oxy-hydroxide materials without an individual phase dominating sufficiently to produce a pattern characteristic of amorphous iron or aluminum (hydrated) oxide. Two peaks at 3.18 and 3.30 Å in the February 2017 sample suggested the possible presence of residual feldspars that had not settled out of suspension.

2.4.1.2 VP-SEM and TIMA3

VP-SEM imaging and TIMA3 elemental mapping of February 2017 and August 2017 NFPS of armored metal-oxyhydroxide cobble coatings qualitatively revealed that NFPS iron content relative to silicon content was higher in February 2017 than in August 2017 (Figures 2.6 - 2.9). Because Fe is a major component of NFCC armored metal-oxyhydroxide cobble coatings (as revealed in elemental analyses, see Section 2.4.1.3), these results suggest that the total amount of armored metal-oxyhydroxide cobble coating relative to the amount of detrital silicate minerals, removed by rock tumbling, decreased after several months of AMD point source treatment. Because stream-bed mineralogy and cobble-coating removal methods did not change between these two timepoints, these data suggest that the combination of several mo of MIW treatment by the North Clear Creek Water Treatment Plant and cobble scouring during spring runoff successfully decreased the amount of metal-oxyhydroxide cobble coatings in NFCC. This conclusion is further supported by results of elemental analyses (Section 2.4.1.3) and visual monitoring (Figure 2.10).

2.4.2 Organism size analyses

To investigate potential impacts of organism size on Cu accumulation and bioavailability, as calculated using the fixed average $[^{63}\text{Cu}]_{\text{b,snail}}$ (Equation 2.1), we first examined the relationship between ^{63}Cu accumulated from NFP over the exposure period ($^{63}\text{Cu}_{\text{accumulated,NFP}}$) and organism size. We identified a negative linear relationship between $^{63}\text{Cu}_{\text{accumulated,NFP}}$ and snail mass, with all organisms >2 mg appearing to have lost ^{63}Cu over the exposure period (Figure 2.11). A loss of ^{63}Cu is interpreted in this method to indicate that an organism did not eat a detectable amount of food over the exposure period. This apparent result

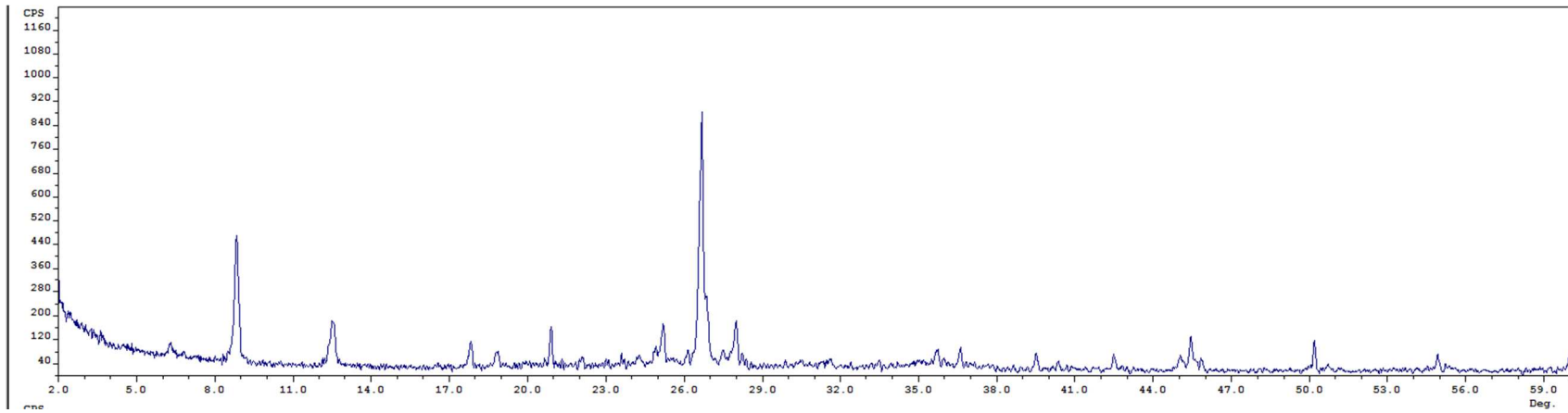


Figure 2.2 X-ray diffraction pattern from an oriented aggregate mount prepared from the <2-mm size fraction of armored coatings removed from cobble collected from the North Fork of Clear Creek in February 2017. The scan was performed from 4-50° 2 theta.

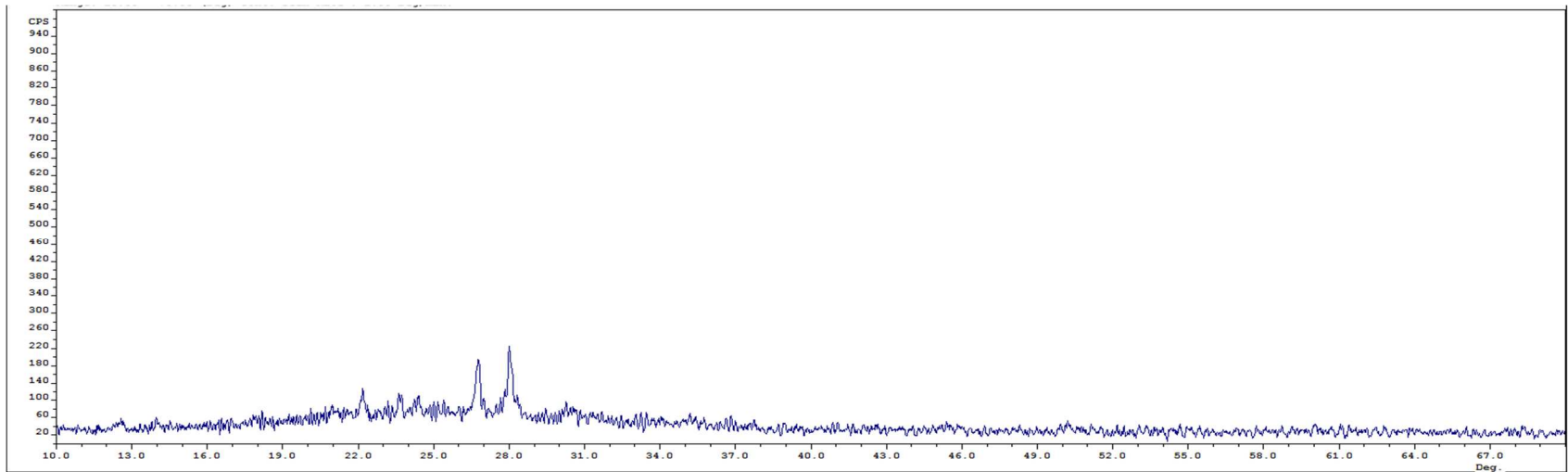


Figure 2.3 X-ray diffraction pattern from an oriented aggregate mount prepared from the <2- μ m size fraction of armored coatings removed from cobble collected from the North Fork of Clear Creek in February 2017. The scan was performed from 4-50° 2 theta.

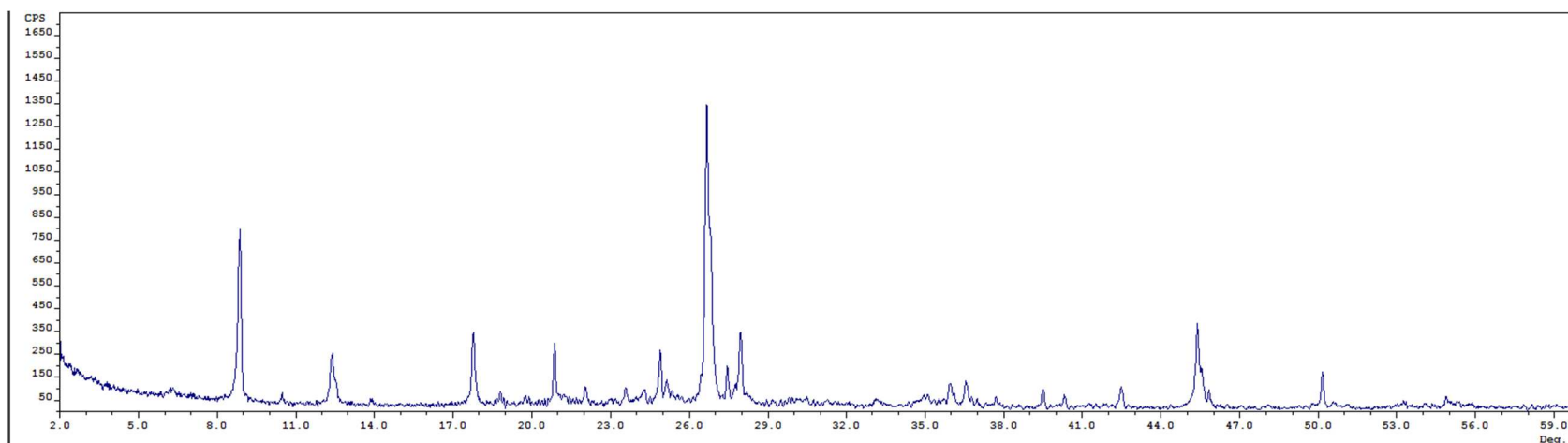


Figure 2.4 X-ray diffraction pattern from an oriented aggregate mount prepared from the <2-mm size fraction of armored coatings removed from cobble collected from the North Fork of Clear Creek in August 2017. The scan was performed from 4-50° 2 theta.

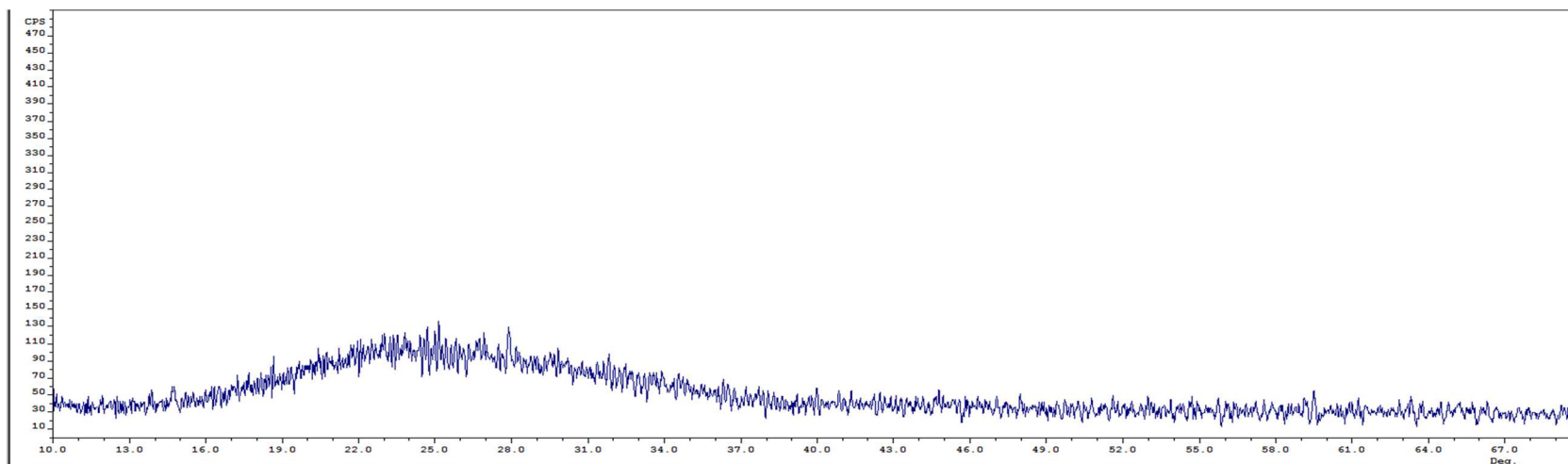


Figure 2.5 X-ray diffraction pattern from an oriented aggregate mount prepared from the <2- μ m size fraction of armored coatings removed from cobble collected from the North Fork of Clear Creek in August 2017. The scan was performed from 4-50° 2 theta.

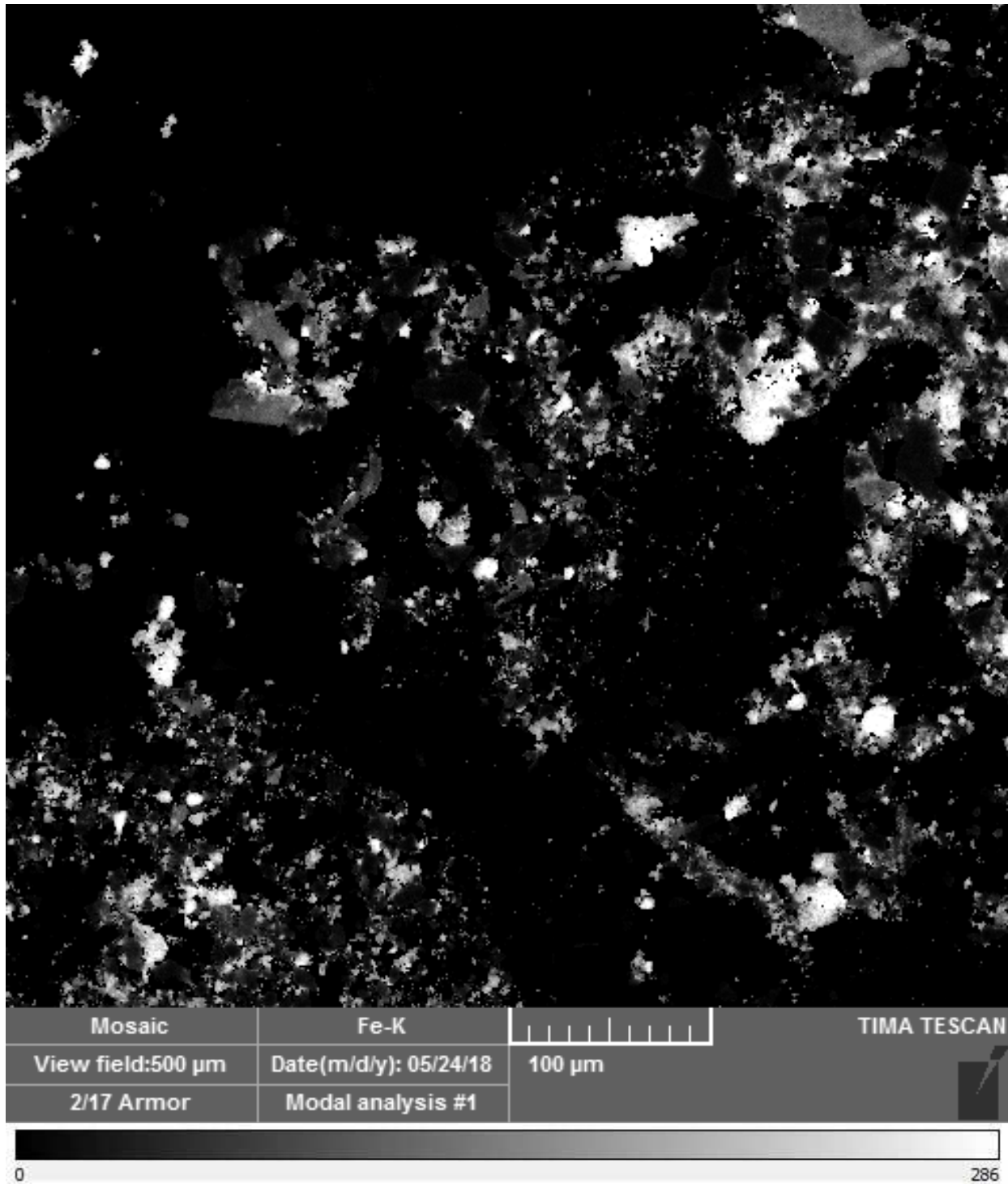


Figure 2.6 Qualitative element map of Fe (K family) dispersal in armored NFCC metal-oxyhydroxide cobble coatings collected in February 2017. Relative Fe concentrations across the sample are indicated by varying degrees of brightness, as determined by element-specific peak intensities measured by VP-SEM.

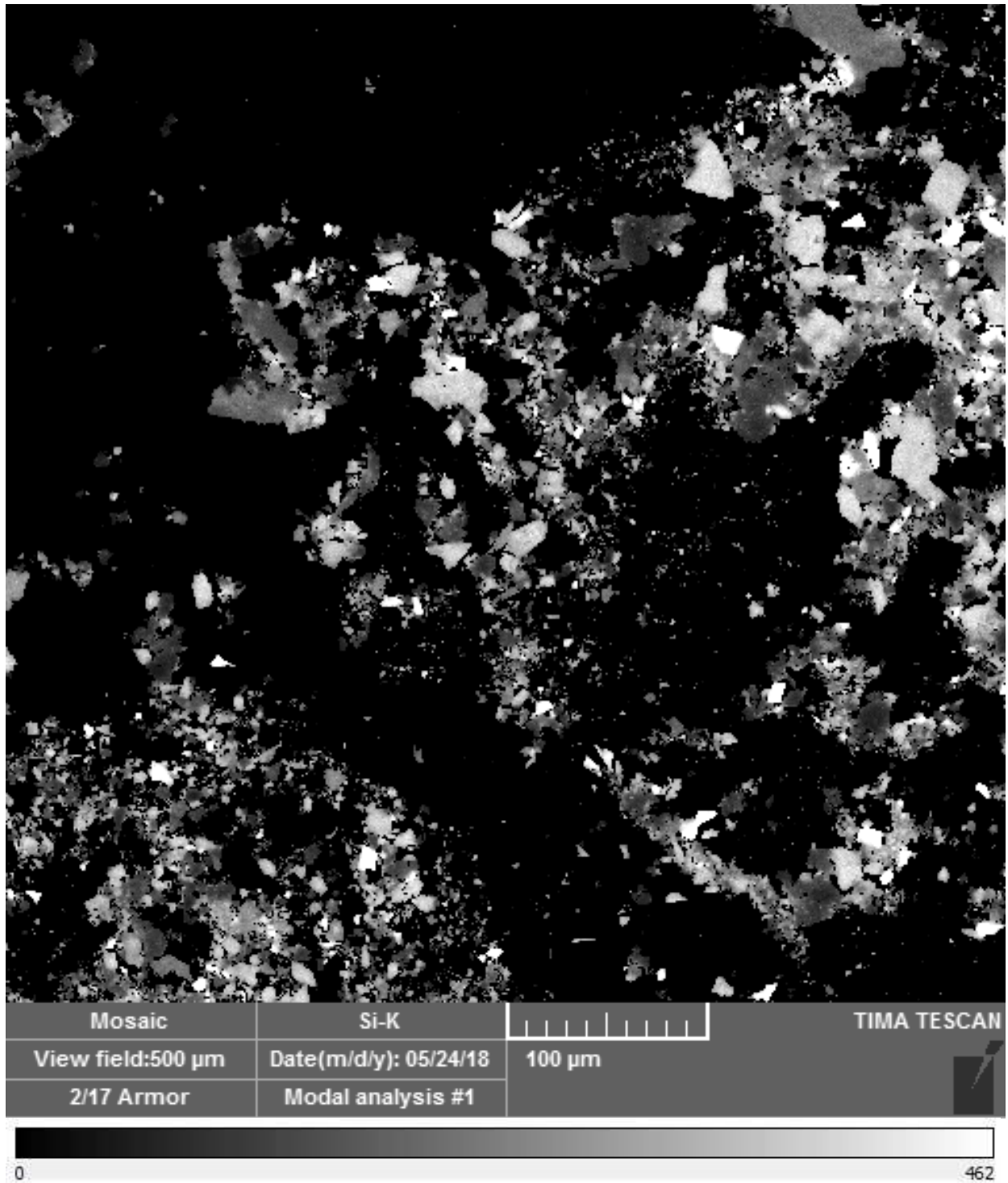


Figure 2.7 Qualitative element map of Si (K family) dispersal in armored NFCC metal-oxyhydroxide cobble coatings collected in February 2017. Relative Si concentrations across the sample are indicated by varying degrees of brightness, as determined by element-specific peak intensities measured by VP-SEM.

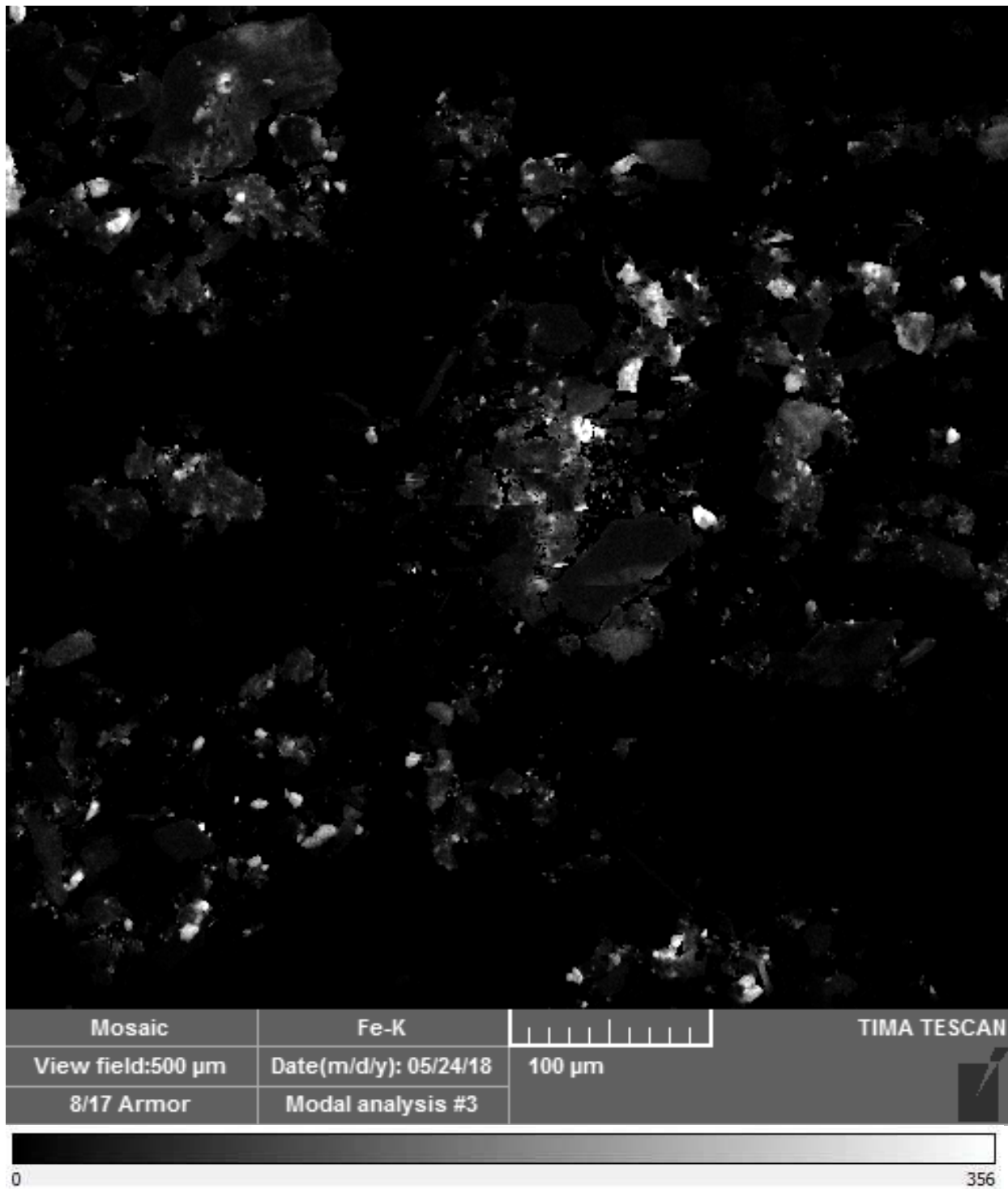


Figure 2.8 Qualitative element map of Fe (K family) dispersal in armored NFCC metal-oxyhydroxide cobble coatings collected in August 2017. Relative Fe concentrations across the sample are indicated by varying degrees of brightness, as determined by element-specific peak intensities measured by VP-SEM.

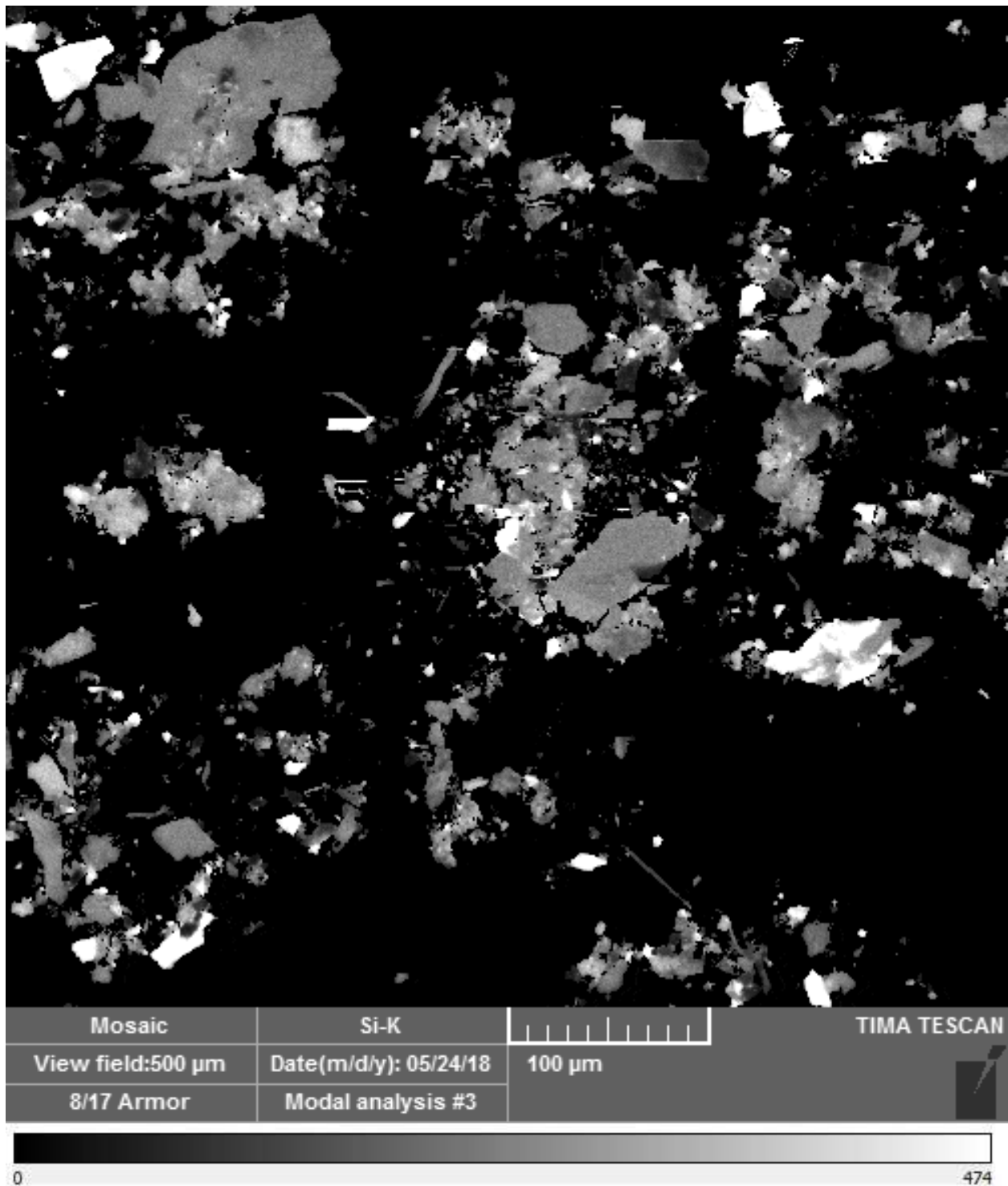


Figure 2.9 Qualitative element map of Si (K family) dispersal in armored NFCC metal-oxyhydroxide cobble coatings collected in August 2017. Relative Si concentrations across the sample are indicated by varying degrees of brightness, as determined by element-specific peak intensities measured by VP-SEM.

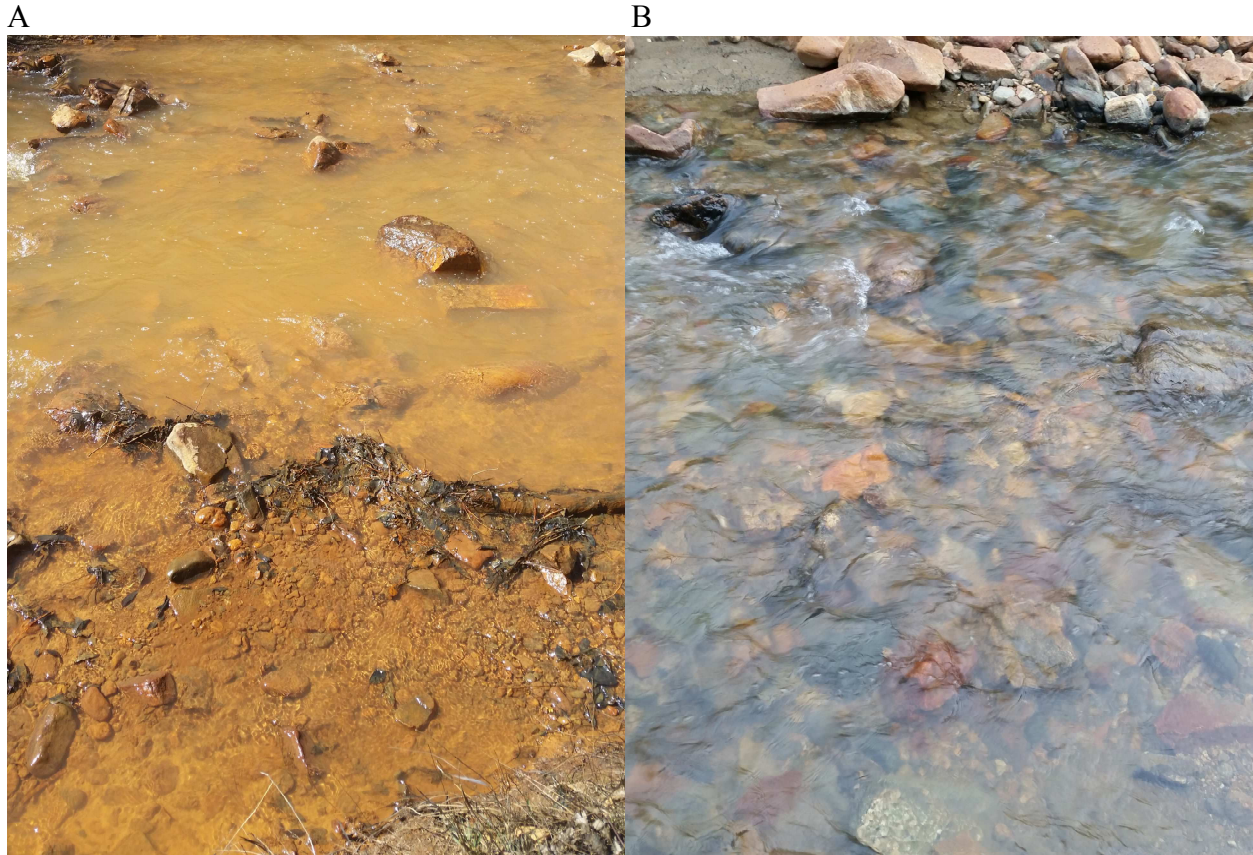


Figure 2.10 Visual monitoring results at the Above Russell Gulch (ARG) site in NFCC in March 2017 (A) and August 2017 (B). March results are pre-treatment, and exhibit cobble heavily coated by metal-oxyhydroxide material. August results are post-treatment, and exhibit cobble scarcely coated by armored metal-oxyhydroxide material.

was suspect for two main reasons: (1) larger organisms (>2 mg) had been observed to be eating and defecating during the experiment and (2) results of a previous experiment in which snails spanning a large size range (0.5-15.2 mg) had been exposed to loose floc removed from NFCC cobble had revealed that organisms should be accumulating more ^{63}Cu with increasing size, due to their ingesting more total food (Appendix A: Supplementary Information).

Because $^{63}\text{Cu}_{\text{accumulated,NFP}}$ is calculated by subtracting $[^{63}\text{Cu}]_{\text{b,snail}}$ and $[^{63}\text{Cu}]_{\text{d-b,snail}}$ from $[^{63}\text{Cu}]_{\text{snail}}$, we next examined the relationship between $[^{63}\text{Cu}]_{\text{snail}}$ values and organism mass to provide insight into the unusual relationship observed between $^{63}\text{Cu}_{\text{accumulated,NFP}}$ and snail mass.

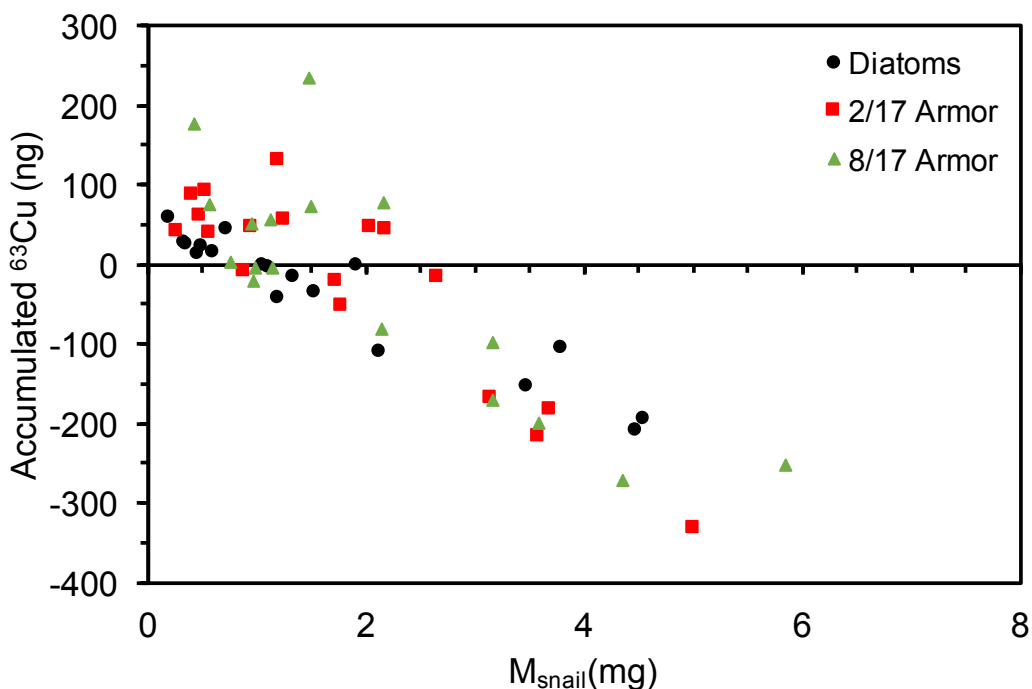


Figure 2.11 ^{63}Cu accumulated by *L. stagnalis* from diatoms, armored cobble coatings from NFCC cobble collected pre-remediation (February 2017) and armored cobble coatings from NFCC cobble collected post-remediation (August 2017), calculated using the average of $^{63}\text{Cu}_{\text{snail}}$ values measured in “background” snails. ^{63}Cu accumulation is organized by organism mass.

In so doing, we found that while larger organisms (>2 mg) all had relatively similar $^{63}\text{Cu}_{\text{snail}}$, $^{63}\text{Cu}_{\text{snail}}$ values increased exponentially with decreasing mass in organisms <2 mg (Figure 2.12).

Upon discovering this trend, we then directly compared the range of $^{63}\text{Cu}_{\text{b,snail}}$ values that we had measured in individual snails with the average $^{63}\text{Cu}_{\text{b,snail}}$ value we had been using for all $^{63}\text{Cu}_{\text{accumulated}}$ calculations (shown in Figure 2.11). This comparison revealed that average $^{63}\text{Cu}_{\text{b,snail}}$ was only a reasonable value for organisms weighing ~ 1 mg, with average $^{63}\text{Cu}_{\text{b,snail}}$ being lower than $^{63}\text{Cu}_{\text{b,snail}}$ measured in organisms <1 mg and higher than $^{63}\text{Cu}_{\text{b,snail}}$ measured in organisms >1 mg.

To allow for the calculation of size-specific $[^{63}\text{Cu}]_{\text{b,snail}}$ values, we then fit a curve to the data for $[^{63}\text{Cu}]_{\text{b,snail}}$ measured in snails spanning a size range of 0.39 mg to 4.95 mg. This analysis revealed that $[^{63}\text{Cu}]_{\text{b,snail}}$ data for the entire size range followed the relationship: $[^{63}\text{Cu}]_{\text{b,snail}} = 70.088 \times M_{\text{snail}}^{-0.628}$. This parameter was substituted into the equation for the total mass of ^{63}Cu accumulated by snails exposed to diatoms only ($^{63}\text{Cu}_{\text{accumulated,d}}$) (Equation 2.3).

$$\begin{aligned} {}^{63}\text{Cu}_{\text{accumulated,d}} &= ([^{63}\text{Cu}]_{\text{snail}} - (70.088 \times M_{\text{snail}}^{-0.628} \\ &+ \frac{k_{\text{ulett}}[^{63}\text{Cu}]_{\text{lett}}}{k_e} (1 - \exp^{-k_e T_2}))) \times M_{\text{snail}} \end{aligned} \quad (2.3)$$

We also observed that tissue concentrations of ^{63}Cu measured in organisms exposed to feeding mats composed of diatoms only ($[^{63}\text{Cu}]_{\text{d,snail}}$) followed a similar size-dependent trend. Because we had also previously used a fixed average of $[^{63}\text{Cu}]_{\text{d,snail}}$ to calculate $^{63}\text{Cu}_{\text{accumulated,NFP}}$, we then fit a curve to the data for $[^{63}\text{Cu}]_{\text{d,snail}}$ measured in snails spanning a size range of 0.2 mg to 4.56 mg. $[^{63}\text{Cu}]_{\text{d,snail}}$ data for the entire size range followed the relationship: $[^{63}\text{Cu}]_{\text{d,snail}} = 80.813 \times M_{\text{snail}}^{-0.663}$. Tissue ^{63}Cu concentrations measured in snails exposed to diatom-only feeding mats include background ^{63}Cu , thus we substituted size-dependent $[^{63}\text{Cu}]_{\text{d,snail}}$ values into our final equation for $^{63}\text{Cu}_{\text{accumulated,NFP}}$ in place of the fixed averages for $[^{63}\text{Cu}]_{\text{d,snail}}$ and $[^{63}\text{Cu}]_{\text{b,snail}}$ (Equation 2.4).

$$\begin{aligned} {}^{63}\text{Cu}_{\text{accumulated,NFP}} &= ([^{63}\text{Cu}]_{\text{snail}} - (80.813 \times M_{\text{snail}}^{-0.663} \\ &+ \frac{k_{\text{ulett}}[^{63}\text{Cu}]_{\text{lett}}}{k_e} (1 - \exp^{-k_e T_2}))) \times M_{\text{snail}} \end{aligned} \quad (2.4)$$

The use of this new parameter enabled us to calculate individual, size-specific $[^{63}\text{Cu}]_{\text{b,snail}}$ values that were more accurate for individuals spanning the range of organism sizes used in the experiment, rather than using an average that was heavily skewed by $[^{63}\text{Cu}]_{\text{snail}}$ values measured

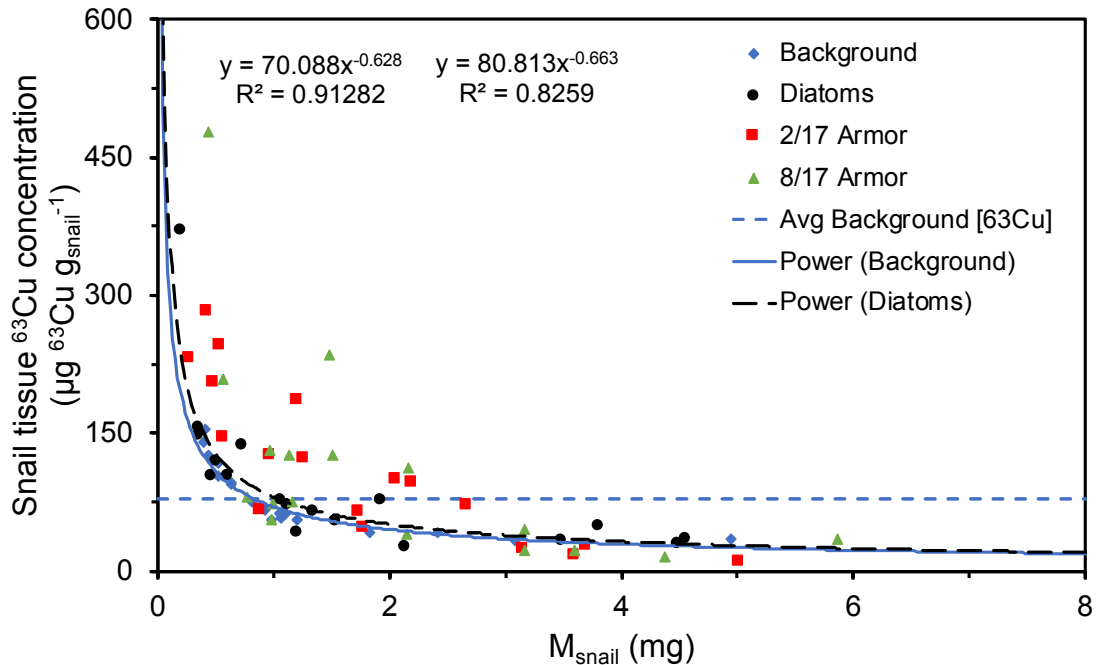


Figure 2.12 Concentrations of ^{63}Cu in soft tissue of *L. stagnalis* not exposed to any material (background), and exposed to diatoms only, diatoms and armored metal-oxyhydroxide cobble coatings from NFCC cobble collected pre-remediation (February 2017), and diatoms and armored metal-oxyhydroxide cobble coatings from NFCC cobble collected post-remediation (August 2017), by organism mass. The dashed blue line represents the average $[\text{}^{63}\text{Cu}]_{\text{b,snail}}$ measured in background snails and used for initial ^{63}Cu accumulation calculations. The smooth black line and corresponding equation represent the curve fit to each $[\text{}^{63}\text{Cu}]_{\text{b,snail}}$ value measured in individual snails and used in size-dependent ^{63}Cu accumulation calculations.

in background organisms weighing <2 mg.

To further investigate the repercussions of our previously using average $[\text{}^{63}\text{Cu}]_{\text{b,snail}}$ in our calculations of $^{63}\text{Cu}_{\text{accumulated,NFP}}$ for the entire range of organism sizes, we compared measured $[\text{}^{63}\text{Cu}]_{\text{b,snail}}$ in “background” organisms, $[\text{}^{63}\text{Cu}]_{\text{b,snail}}$ in experimental organisms, and average $[\text{}^{63}\text{Cu}]_{\text{b,snail}}$. This analysis (as shown in Figure 2.12) revealed that for organisms <1 mg, calculations using average $[\text{}^{63}\text{Cu}]_{\text{b,snail}}$ had resulted in the apparent accumulation of unrealistically high masses of ^{63}Cu during the exposure period. Additionally, organisms >1 mg appeared to have accumulated unrealistically low, or even negative, masses of ^{63}Cu . This issue was magnified for organisms >2 mg, for which measured $[\text{}^{63}\text{Cu}]_{\text{snail}}$ for all but 3 organisms ranged

between 11.5 and 71.8 $\mu\text{g } ^{63}\text{Cu g}_{\text{snail}}^{-1}$, which is well below the average $[\text{}^{63}\text{Cu}]_{\text{b,snail}}$ value of 77.9 $\mu\text{g } ^{63}\text{Cu g}_{\text{snail}}^{-1}$. A comparison of average $[\text{}^{63}\text{Cu}]_{\text{b,snail}}$ and size-specific $[\text{}^{63}\text{Cu}]_{\text{b,snail}}$ values calculated from the curve fit to $[\text{}^{63}\text{Cu}]_{\text{snail}}$ values measured in “background” snails is summarized in Appendix A.

Following the re-calculation of $^{63}\text{Cu}_{\text{accumulated,NFP}}$ for experimental organisms using size-specific $[\text{}^{63}\text{Cu}]_{\text{b,snail}}$ values, we re-examined the relationship between $^{63}\text{Cu}_{\text{accumulated,NFP}}$ and organism mass. This analysis revealed that there continued to be a slightly negative linear relationship between $^{63}\text{Cu}_{\text{accumulated,NFP}}$ and organism size (Figure 2.13). Organisms <3 mg accumulated much more ^{63}Cu from feeding mats comprising mixtures of diatoms and NFP than they did from feedings mats composed of diatoms only. Organisms >3 mg, conversely, only accumulated ^{63}Cu when exposed to feeding mats composed of diatoms only, and lost ^{63}Cu when exposed to feeding mats comprising mixtures of diatoms and NFP. Concentrations of ^{63}Cu in feeding mats containing diatoms only were relatively high ($\sim 275 \mu\text{g } ^{63}\text{Cu g}_{\text{mat}}^{-1}$), but concentrations of ^{63}Cu in feeding mats composed of mixtures of diatoms and NFP were not dramatically higher than in mats composed of diatoms only ($357 \mu\text{g } ^{63}\text{Cu g}_{\text{mat}}^{-1}$ in February 2017 NFP and $387 \mu\text{g } ^{63}\text{Cu g}_{\text{mat}}^{-1}$ in August 2017 NFP). The observed size-dependent trends for ^{63}Cu accumulation suggest, therefore, that organisms >3 mg were not eating feeding on mats composed of mixtures diatoms and NFP, while organisms <3 mg may have been preferentially feeding on mats composed of mixtures of diatoms and NFP. The underlying causes of these observed feeding patterns is not known.

Analyses of tissue ^{65}Cu concentrations in background snails ($[\text{}^{65}\text{Cu}]_{\text{b,snail}}$) revealed that there was no clearly defined relationship between $[\text{}^{65}\text{Cu}]_{\text{b,snail}}$ and organism mass in organisms <2

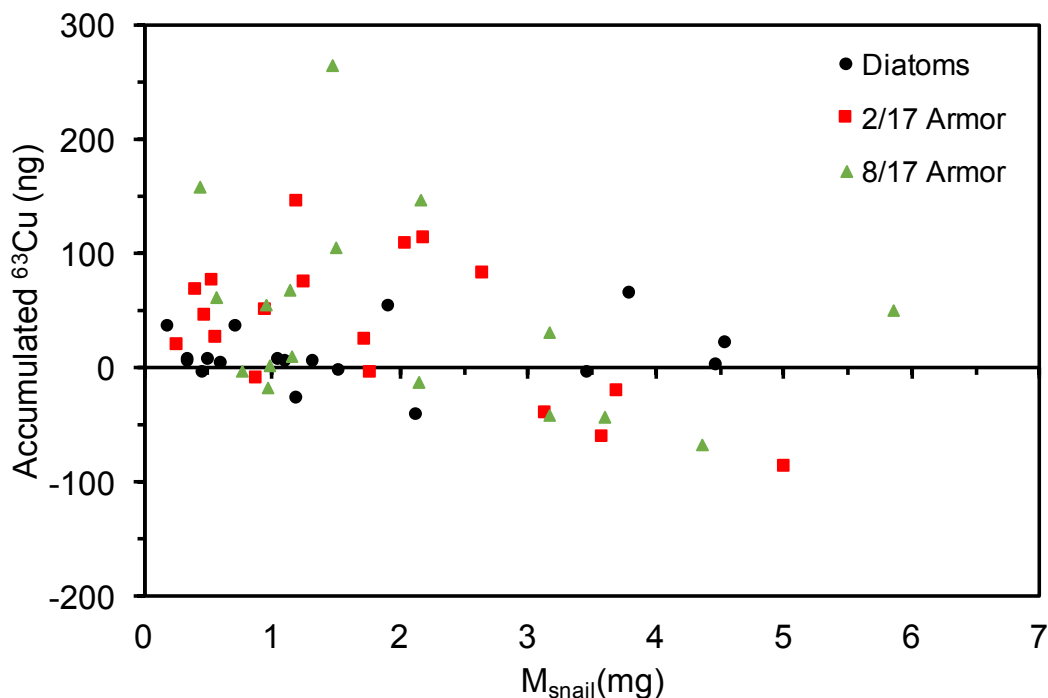


Figure 2.13 ^{63}Cu accumulated by *L. stagnalis* from diatoms, armored metal-oxyhydroxide cobble coatings from NFCC cobble collected pre-remediation (February 2017), and armored metal-oxyhydroxide cobble coatings from NFCC cobble collected post-remediation (August 2017), calculated using size-specific $[\text{Cu}]_{\text{b,snail}}$ values (Equation 2.13 for diatom-fed snails, and Equation 2.14 for diatom and NFP-fed snails). ^{63}Cu accumulation is organized by organism mass.

mg (Figure 2.14). In organisms >2 mg, $[\text{Cu}]_{\text{b,snail}}$ increased with increasing size. Due to the small number of organisms in this size range ($n = 4$), the relationship between the two parameters could not be conclusively identified as exponential or linear.

Analyses of total tissue Cu concentrations in organisms revealed a size-dependence similar to that identified for $[\text{Cu}]_{\text{snail}}$ (Figure 2.15). $[\text{Cu}]_{\text{snail}}$ was higher in organisms <2 mg and increased exponentially with decreasing size. $[\text{Cu}]_{\text{snail}}$ in organisms >2 mg fell below tissue Cu concentrations measured in background organisms, suggesting that the larger organisms were losing Cu during the exposure. Because Cu is a micronutrient that *L. stagnalis* regulate very

effectively, we would not expect to observe changes in total tissue Cu content over a short exposure period (4 h). More research is needed to determine the cause of this unexpected trend.

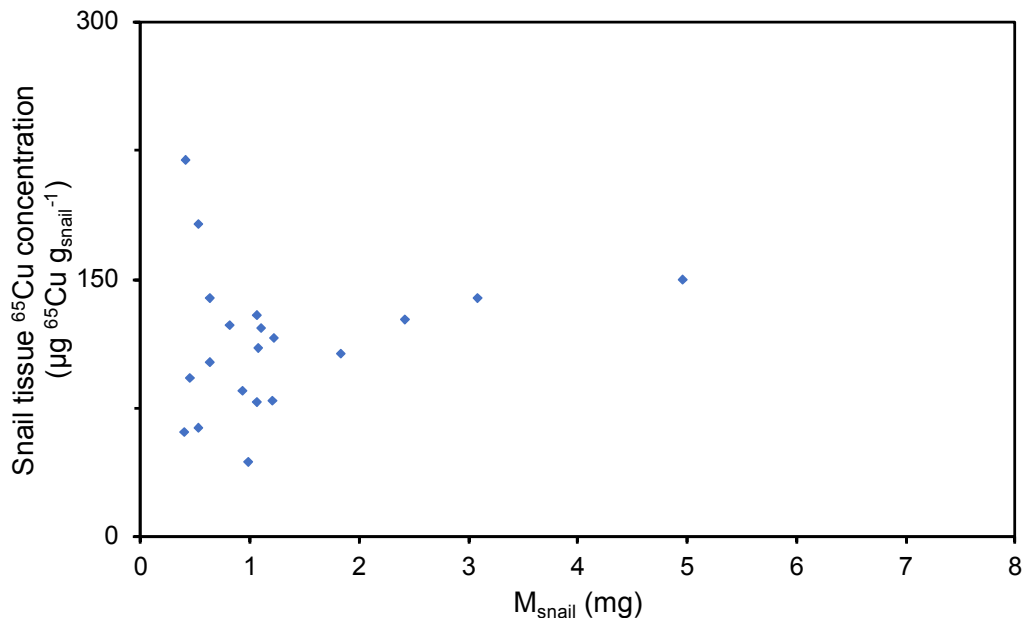


Figure 2.14 Background tissue ⁶⁵Cu concentrations measured in *L. stagnalis* not exposed to diatoms or North Fork Particles (NFP).

Ratios of ⁶⁵Cu to ⁶³Cu in background snails increased with increasing size (Figure 2.16). Several organisms weighing <1 mg had Cu isotope ratios at or near natural abundance, despite having been in ⁶⁵Cu-enriched water for ~4 weeks. For reasons yet unknown, organisms weighing <3 mg do not appear to reverse their Cu isotopic signature as effectively as organisms weighing >3 mg. Because all snails used in this experiment were nearly the same age (within 1-2 weeks post-hatching at the beginning of the isotope-reversal period), the observed size differences suggest variable growth rates between organisms. We suspect that the observed size-related trend in ⁶⁵Cu:⁶³Cu in background snails is due to these variable growth rates. Smaller organisms may have isotope ratios at or near natural abundance due to their growing more slowly, and therefore

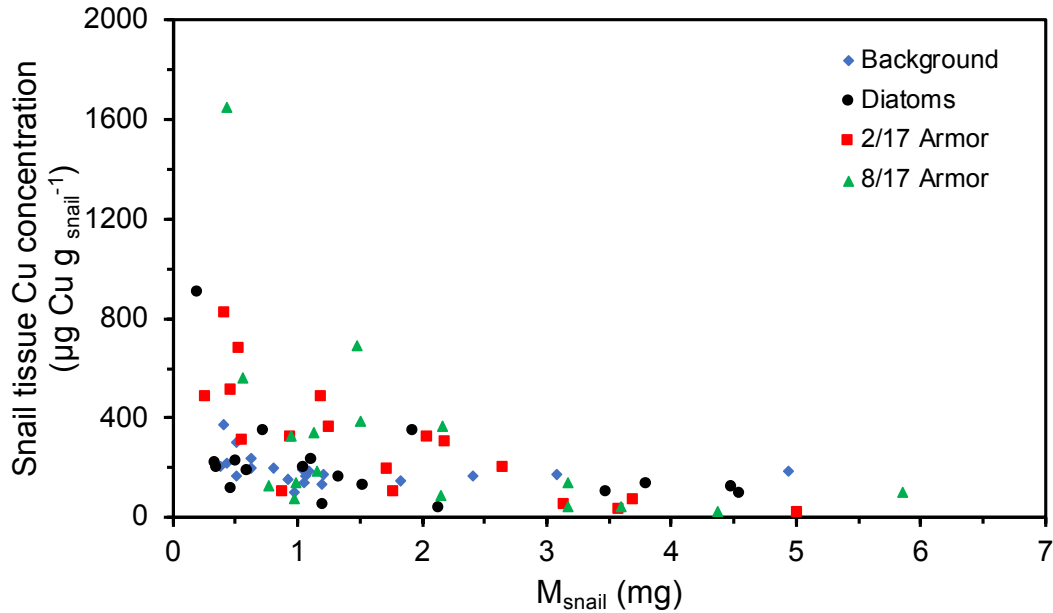


Figure 2.15 Concentrations of total Cu in soft tissue of *L. stagnalis* not exposed to any material (background), and exposed to diatoms only, diatoms and armored metal-oxyhydroxide cobble coatings from NFCC cobble collected pre-remediation (February 2017), and diatoms and armored metal-oxyhydroxide cobble coatings from NFCC cobble collected post-remediation (August 2017), by organism mass.

incorporating less ^{65}Cu into their tissues during the reversal period. Additional work is needed to test this hypothesis.

2.4.3 Copper bioavailability pre- and post-remediation

To determine Cu bioavailability in armored metal-oxyhydroxide cobble coatings removed from NFCC sediments, we first examined average $^{63}\text{Cu}:$ ^{65}Cu in snails not exposed to any material (i.e., “background” snails) and exposed to diatoms only, a mixture of diatoms and NFPS removed from cobble collected in February 2017, and a mixture of diatoms and NFPS removed from cobble collected in August 2017 (Figure 2.17). This analysis showed that isotope ratios in snails exposed to armored NFCC cobble coatings collected on both dates did not differ significantly. Additionally, we observed that isotope ratios in snails exposed to diatoms only did not differ significantly from those in snails exposed to armored cobble coatings from both dates.

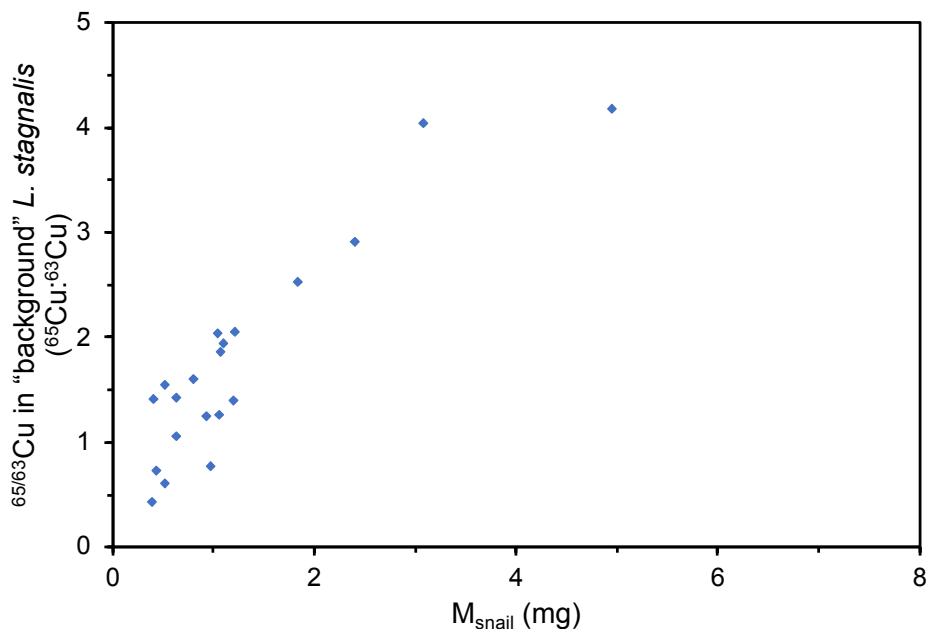


Figure 2.16 Background ratios of ⁶⁵Cu to ⁶³Cu in *L. stagnalis* not exposed to diatoms or North Fork Particles (NFP).

Cu AE calculated using $[\text{}^{63}\text{Cu}]_{\text{b,snail}}$ (Equation 2.2) for snails exposed to armored metal-oxyhydroxide coatings removed from NFCC cobble collected pre- (February 2017) and post-remediation (August 2017) did not differ significantly when investigated simultaneously (Figure 2.18). AE for snails exposed to February 2017 metal-oxyhydroxide coatings was $31.2\% \pm 7.5\%$ (average AE \pm 95% confidence), while that for snails exposed to August 2017 metal-oxyhydroxide coatings was $24.9\% \pm 16.7\%$. Because snails having negative ${}^{63}\text{Cu}_{\text{accumulated,NFP}}$ are assumed to have not eaten detectable amounts of food, those snails were not included in final AE calculations.

AE for snails exposed to February 2017 armored metal-oxyhydroxide coatings recalculated using size-specific $[\text{}^{63}\text{Cu}]_{\text{b,snail}}$ and $[\text{}^{63}\text{Cu}]_{\text{d,snail}}$ (Equation 2.4) was $31.0\% \pm 5.8\%$ (average AE \pm 95% confidence), and AE for snails exposed to August 2017 armored metal-oxyhydroxide coatings was $22.9\% \pm 9.8\%$ (Figure 2.19). Although the 95% confidence interval

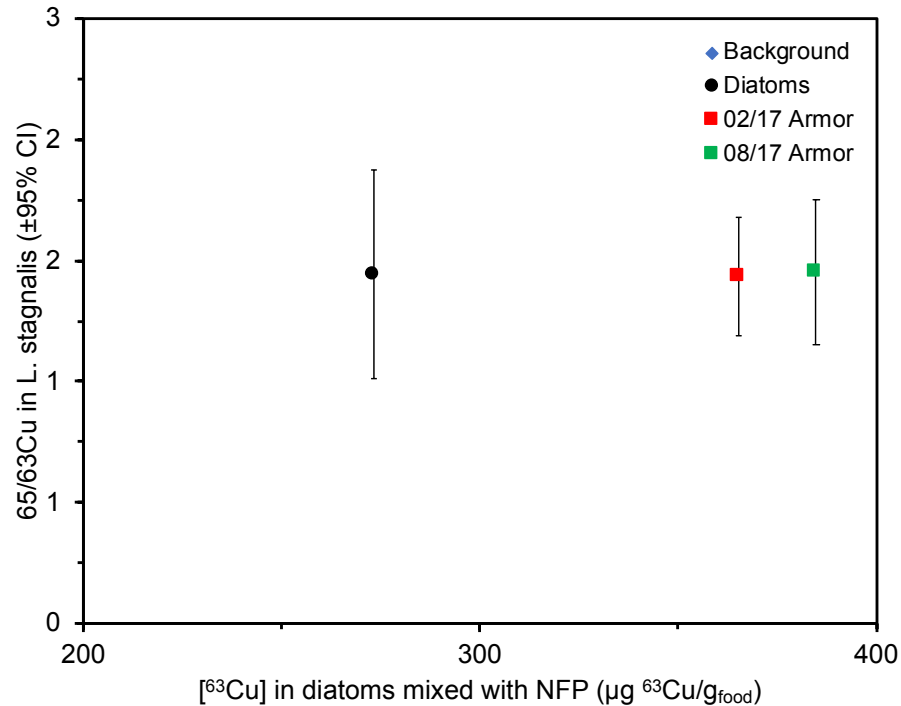


Figure 2.17 $^{65}\text{Cu}:$ ^{63}Cu measured in *L. stagnalis* exposed to mixtures of diatoms and armored cobble coating particles removed from North Fork Clear Creek (NFCC) cobble collected in February 2017 (pre-remediation, n=18) and August 2017 (post-remediation, n=18). Background value was obtained from analysis of 20 snails not exposed to feeding mats.

for Cu AE in snails exposed to February 2017 cobble coatings was smaller than that resulting from our original calculations using Equation 2.2 ($\pm 7.5\%$ versus $\pm 5.8\%$), the 95% confidence interval for snails exposed to August 2017 cobble coatings remained virtually unchanged ($\pm 9.1\%$ versus $\pm 9.8\%$). These data suggest that there may have been a source of considerable error in addition to the range of organism sizes used, or that the improvements made to our calculations were not sufficient to substantially reduce the overall between-organism variability in our end results. Most importantly, Cu bioavailability in armored metal-oxyhydroxide cobble coatings from NFCC still did not differ significantly pre- and post-remediation.

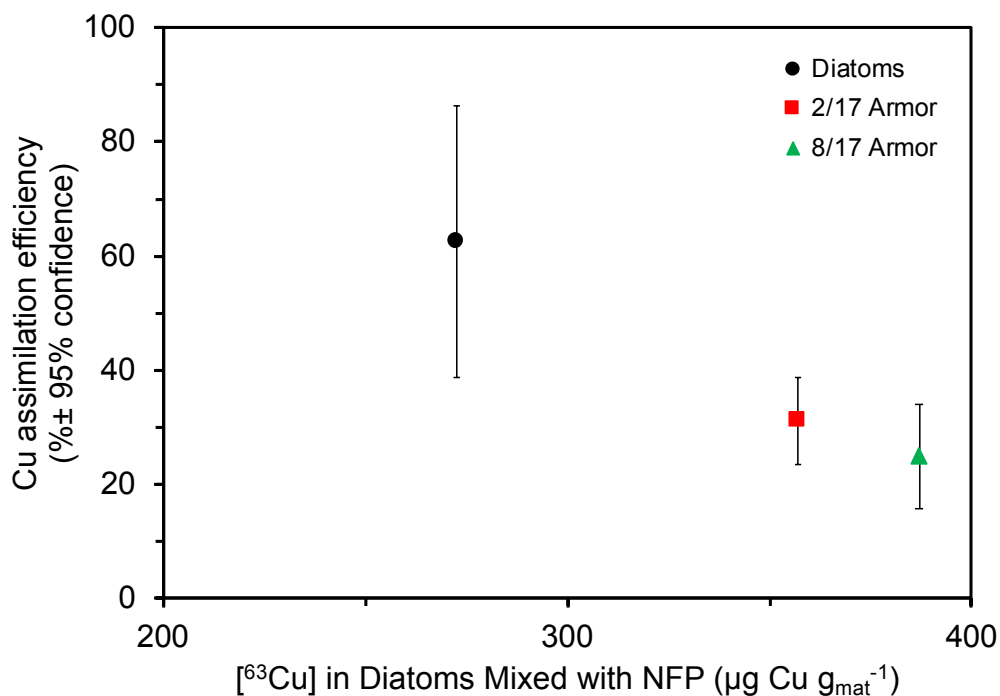


Figure 2.18 Assimilation efficiency (AE) of ⁶³Cu by *L. stagnalis* exposed to diatoms only (n = 6) and armored metal-oxyhydroxide cobble coating particles removed from North Fork Clear Creek (NFP) cobble collected in February 2017 (pre-remediation, n = 10) and August 2017 (post-remediation, n = 8) calculated using fixed averages of tissue ⁶³Cu concentrations measured in “background” snails and snails exposed to diatoms only (Equation 2.2). Diatom-particle feeding mats were prepared for target total [Cu] of 0 (Diatoms) and 600 µg Cu g⁻¹ food (2/17 Armor and 8/17 Armor). Background ⁶³Cu used in the calculation was the average of values measured in 18 organisms. Error bars represent a 95% confidence interval.

2.5 Synthesis

Mining-influenced waters are a complex and widespread environmental issue plaguing many rivers across the Western United States. Although the environmental impacts of MIW are well documented, the responses of MIW to remediation are less understood. Although recent studies including the work of Clements et al.³ have increased the understanding of biological and physicochemical responses of MIW to remediation, potential changes to dietborne metal bioavailability in MIW during treatment have mostly remained unstudied. The results reported

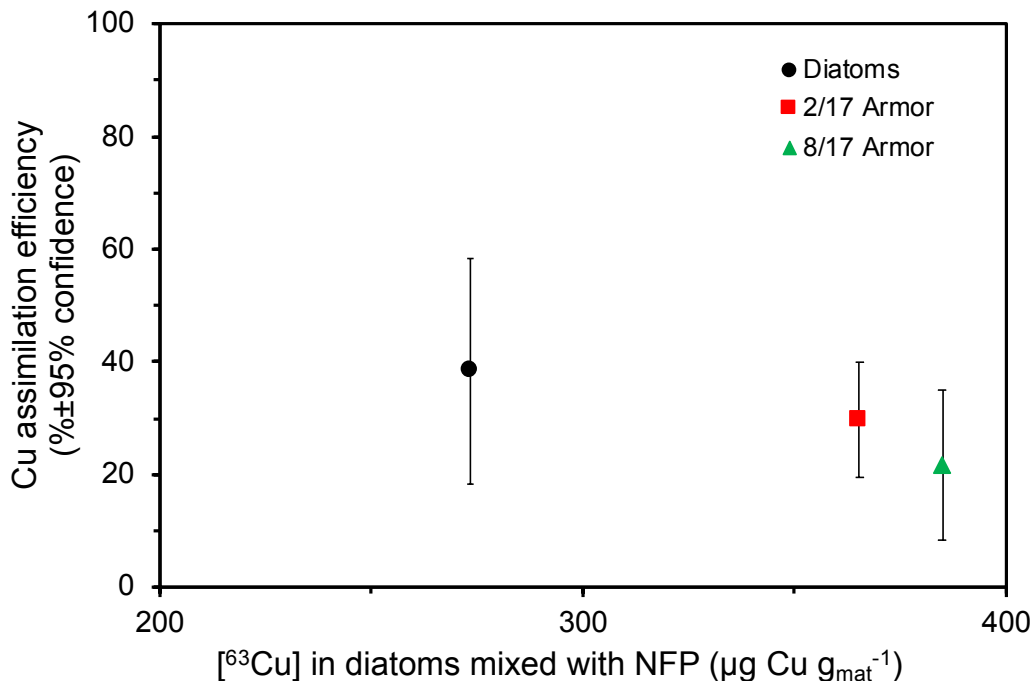


Figure 2.19 Assimilation efficiency (AE) of ⁶³Cu in *L. stagnalis* exposed to diatoms only (n = 13) and armored metal-oxyhydroxide cobble coating particles removed from North Fork Clear Creek (NFP) cobble collected in February 2017 (pre-remediation, n = 12) and August 2017 (post-remediation, n = 11), re-calculated using size-specific [⁶³Cu]_{b,snail} and [⁶³Cu]_{d,snail} values (Equation 2.4). Diatom-particle feeding mats were prepared for target total [Cu] of 0 (Diatoms) and 600 µg Cu g⁻¹ food (2/17 Armor and 8/17 Armor). Error bars represent a 95% confidence interval.

herein indicate first and foremost that Cu bioavailability in armored metal-oxyhydroxide cobble coatings collected from NFCC did not differ significantly pre- and post-remediation. This finding, in addition to results of cobble coating characterizations of pre- and post-remediation cobble coatings, suggests that the composition of armored metal-oxyhydroxide cobble coatings in a section of NFCC where concentrations of metals and water chemistry have changed

substantially (Appendix A) has not been altered over time. However, further analysis of Cu speciation in armored metal-oxyhydroxide cobble coatings would need to be performed to test this hypothesis.

Additionally, although snails were a logical choice of organism due to their wide use in bioavailability experiments similar to ours, they are not ecologically relevant to the high-gradient, montane streams typically impacted by MIW in Colorado. Results of this work, therefore, may not accurately represent metal bioavailability in this type of ecosystem. However, larval gut pH in two chironomid species were circumneutral,¹⁶ as in *L. stagnalis*.¹⁷ Although Cu bioavailability is likely not identical in *Chironomidae* and *L. stagnalis*, they may be similar.

Given that invertebrates native to montane streams are typically smaller than freshwater snails, we used a range of small organism sizes to work towards establishing organism-size constraints of reverse-labeling, stable isotope bioavailability studies, as well as to determine if the adaptation of such methods to smaller invertebrate species will be feasible. In organisms weighing <2 mg, $[^{63}\text{Cu}]_{\text{snail}}$ and $[\text{Cu}]_{\text{snail}}$ decreased exponentially with increasing snail mass. A slightly negative correlation between tissue metal concentrations and organism mass would be expected in the case of a micronutrient (e.g., Cu in *L. stagnalis*), due to the combined effects of equilibration (balance of metal influx and efflux rates) and growth dilution,¹⁸ however the observed exponential correlation, particularly in the case of $[^{63}\text{Cu}]_{\text{snail}}$, suggested that additional factors were influencing our results. Williamson¹⁹ reported a similar but less dramatic correlation between lead (Pb) and Zn concentrations in the terrestrial snail *Capaea hortensis*, coming to the conclusion that elevated tissue metal concentrations in small snails were the result of high metabolic activity in those smaller organisms. Such high metabolic activity is a possible cause of the correlation between $[^{63}\text{Cu}]_{\text{snail}}$ and organism mass that we observed in *L. stagnalis* as well.

Because the same correlation was observed in both background and experimental snails, it is possible that snails weighing <2 mg were ingesting much higher amounts of Cu per unit organism mass than snails weighing >2 mg. Additionally, the efflux rates in smaller organisms likely did not match their influx rates at their early stage of development.¹⁹

An additional likely factor in the observed size-dependent trend in $[^{63}\text{Cu}]_{\text{snail}}$ values was that organisms <3 mg did not appear to reverse their isotopic signatures over the 4-week period. A failure to reverse would result in higher initial ^{63}Cu concentrations and isotopic ratios closer to natural abundance in smaller snails. This result suggests that smaller snails may not have been exchanging ^{63}Cu for ^{65}Cu , for reasons yet unknown. Because a similar, though less dramatic, correlation was observed between $[\text{Cu}]_{\text{snail}}$ and organism mass, failure to reverse was not the only cause of the observed size-dependent $[^{63}\text{Cu}]_{\text{snail}}$ values. Without further research, it is not possible to determine if the snails' failure to become enriched in ^{65}Cu is the result of slow growth rates (slower rates of growth could result in slower rates of ^{65}Cu accumulation into soft tissue) or another unidentified mechanism.

Finally, organisms >3 mg appeared to be losing total Cu over the exposure period. Further work is needed to determine whether those snails actually lost Cu, or if an unidentified factor may have increased measured $[\text{Cu}]_{\text{snail}}$ in background organisms (e.g., residual lettuce in their guts) resulting in an apparent net loss of Cu in organisms that have fully depurated.

In addition to high metabolic activity in small organisms, a possible additional factor in producing the organism-size trends observed herein may be organism growth rates. Zotin²⁰ reported that *L. stagnalis* exhibit an exponential growth rate in organisms <3 mg. Such exponential growth could result in exponential growth dilution (i.e., tissue metals concentrations decreasing exponentially with increasing organism size), further obscuring metal accumulation

data. Such a result would be dependent on metal influx and growth rates, which in this experiment varied between organisms, requiring that tissue growth rates exceeded influx rates. Further analysis is needed to determine whether this type of effect influenced our results.

We suggest, therefore, that in determining organism-size constraints for bioavailability studies, only organisms that have achieved a size at which both feeding and growth rates have stabilized be used. While we were able to generate size-dependent equations for working with small snails, the ramifications of small measurement errors when working with organisms in early stages of development are substantial. Errors in mass measurements of as little as ± 0.1 mg, for example, can produce dramatically different results in background tissue metal concentrations, final tissue metal concentrations, and, consequently, metal accumulation. Because early post-hatching growth and metal accumulation rates vary between both organisms²¹ and metals,¹⁹ such determinations of size constraints will need to be made specifically for the organism and metal of interest.

Additionally, we recommend that only organisms developing at similar growth rates (i.e., hatched at the same time, and grown to the same size) be used in bioavailability studies to reduce sources of between-organism variability.

2.6 Acknowledgements

We extend our thanks to Elizabeth Traudt for her training in this method, Marie-Noële Croteau for her aid in interpreting results, and Katharina Pfaff for her assistance with VP-SEM analyses. This research was supported by the National Institute of Environmental Health Sciences (1R01ES024358) and the International Zinc Association (ETAP201).

2.7 References

(1) Watkins, T. H. Hard rock legacy. *National Geographic*, Mar. 2000, 197(3).

- (2) Mittal, A. K. *Abandoned mines: information on the number of hardrock mines, cost of cleanup, and value of financial assurances*; GAO-11-834T; United States Government Accountability Office: Washington, 2011; www.gao.gov/assets/130/126667.pdf.
- (3) Clements, W. H.; Vieira, N. K.; Church, S. E. Quantifying restoration success and recovery in a metal-polluted stream: a 17-year assessment of physicochemical and biological responses. *J. Appl. Ecol.* **2010**, 47(4), 899-910; DOI 10.1111/j.1365-2664.2010.01838.x.
- (4) Cox, T. *Inside the Mountains: A History of Mining Around Central City, Colorado*; Pruett Publishing Company: Boulder, CO, 1989.
- (5) Jessen, K. The Deadly End to the Argo Tunnel. *The Loveland Reporter-Herald*, Sep. 18, 2011.
- (6) *Grand Opening Fact Sheet: Central City/Clear Creek Superfund Site*; Colorado Department of Public Health and Environment, Denver, CO, 2017.
- (7) Croteau, M.-N.; Cain, D. J.; Fuller, C. C. Novel and nontraditional use of stable isotope tracers to study metal bioavailability from natural particles. *Environ. Sci. Technol.* **2013**, 47, 3424-3431; DOI 10.1021/es4000162f.
- (8) Sprong, N.; Brinkman, F. G.; Van Hoek, R. J.; Knook, D. L. Copper in *Lymnaea stagnalis* L.-II. effect on the kidney and body fluids. *Comp. Biochem. Physiol.* **1971**, 38A, 309-316; DOI 10.1016/0300-9629(71)90057-0.
- (9) Balance, S.; Phillips, P. J.; McCrohan, C. R.; Powell, J. J.; Jugdaohsingh, R.; White, K. N. Influence of cobble biofilm on the behaviour of aluminum and its bioavailability to the snail *Lymnaea stagnalis* in neutral freshwater. *Can. J. Fish. Aquat. Sci.* **2001**, 58 (9), 1708-1715; DOI 10.1139/f01-104.
- (10) Coeurdassier, M.; De Vaufleury, A.; Badot P. -M. Bioconcentration of cadmium and toxic effects on life-history traits of pond snails (*Lymnaea palustris* and *Lymnaea stagnalis*) in laboratory bioassays. *Arch. Environ. Contam. Toxicol.* **2003**, 45 (1), 102-109; DOI 10.1007/s00244-002-0152-4.
- (11) Lewis, P. A.; Klemm, D. J.; Lazorchak, J. M.; Norberg-King, T. J.; Peltier, W. H.; Heber, M. A. *Short-Term Methods for Estimating the Chronic Toxicity of Effluents and Receiving Waters to Freshwater Organisms, Third Edition*; Technical Report EPA-600-4-91-002; United States Environmental Protection Agency, Environmental Monitoring and Support Laboratory: Cincinnati, OH, 1994.
- (12) Zeisler, R.; Murphy, K. E.; Becker, D. A.; Davis, W. C.; Kelly, W. R.; Long, S. E.; Sieber, J. R. Standard Reference Materials® (SRMs) for measurement of inorganic environmental contaminants. *Anal. Bioanal. Chem.* **2006**. 386 (4), 1137–1151; DOI 10.1007/s00216-006-0785-7.

- (13) Croteau, M. N.; Luoma, S. N. A biodynamic understanding of dietborne metal uptake by a freshwater invertebrate. *Environ. Sci. Technol.* **2008**, 42 (5), 1801–1806; DOI 10.1021/es7022913.
- (14) Moore, D. M.; Reynolds, R. C. *X-ray Diffraction and the Identification and Analysis of Clay Minerals*, Oxford University Press: Oxford, U.K., 1997.
- (15) *Method 3051A*, United States Environmental Protection Agency: Washington, DC, 2007; www.epa.gov/sites/production/files/2015-12/documents/3051a.pdf.
- (16) Frouz, J.; Lobinske, R. J.; Yaqub, A.; Ali, A. Larval gut pH profile in pestiferous *Chironomus crassicaudatus* and *Glyptotendipes paripes* (Chironomidae: Diptera) in reference to the toxicity potential of *Bacillus thuringiensis* serovar *Israelensis*. *J. Am. Mosq. Control Assoc.* **2007**, 23 (3), 355-358; DOI 10.2987/8756-971X(2007)23[355:LGPPIP]2.0.CO;2.
- (17) Carriker, M. R. Observations on the functioning of the alimentary system of the snail *Lymnaea stagnalis appressa* Say. *Biol. Bull.* **1946**, 91, 88-111; DOI 10.2307/1538036.
- (18) Strong, C. R.; Luoma, S. N. Variations in the correlation of body size with concentrations of Cu and Ag in the bivalve *Macoma balthica*. *Can. J. Fish. Aquat. Sci.* **1981**, 38, 1059-1064; DOI 10.1139/f00-042.
- (19) Williamson, P. Variables affecting body burdens of lead, zinc, and cadmium in a roadside population of the snail *Capaea hortensis* Müller. *Oecologia.* **1980**, 44 (2), 213-220; DOI 10.1007/BF00572682.
- (20) Zotin, A. A. Individual growth of *Lymnaea stagnalis* (Lymnaeidae, Gastropoda): II. late postlarval ontogeny. *Biol. Bull.* **2009**, 36 (6), 591-597; DOI 10.1134/S1062359009060077.
- (21) Zotin, A. A. The growth and energy metabolism of *Lymnaea stagnalis* (Lymnaeidae, Gastropoda): I. early postlarval period. *Biol. Bull.* **2009**, 36 (5), 455-463. DOI 10.1134/S1062359009050057.

CHAPTER 3

SUMMARY AND CONCLUSIONS

3.1 Summary of results and implications

Mining influenced waters (MIW) are an extremely complex and widespread environmental issue that contaminate an estimated 40% of Western United States headwaters.¹ Although many studies have been conducted to examine the generation and environmental impacts of MIW, little is known about potential changes to dietborne metal bioavailability in MIW during remediation. Following the construction of a high-density sludge (HDS) lime treatment plant on the North Fork of Clear Creek (NFCC) in Black Hawk, Colorado,² I addressed this information gap by examining if copper (Cu) bioavailability in metal-oxyhydroxide cobble coatings, which are characteristic of MIW-impacted sites, changes during remediation. Using an adaptation of a reverse-labeling, stable-isotope method devised by Croteau et al.,³ I concluded that Cu bioavailability in freshwater snails (*Lymnaea stagnalis*) exposed to armored metal-oxyhydroxide cobble coatings from NFCC did not differ significantly pre- and post-remediation.

Although the results of the *L. stagnalis* bioavailability experiments were informative, they might not provide the most accurate estimate of Cu bioavailability in NFCC. Freshwater snails are not native to high-gradient, montane streams like NFCC, and Cu assimilation efficiency (AE) in aquatic macroinvertebrates that are more relevant to montane streams could differ from AE measured in snails. Because invertebrates relevant to these types of ecosystems are generally smaller than snails that have been used in previous bioavailability experiments, I used organisms spanning a range of small dry tissue masses (~0.5-5 mg) in my experiment to test the suitability of this method for use with smaller species. Results of these organism-size

analyses revealed that tissue ^{63}Cu concentrations in both “background” and test organisms weighing <2 mg increased exponentially with decreasing mass.

High measured background tissue ^{63}Cu concentrations ($[\text{}^{63}\text{Cu}]_{\text{b,snail}}$) in smaller organisms created extreme difficulty in calculating total ^{63}Cu accumulated over background ($^{63}\text{Cu}_{\text{accumulated}}$) during the exposure period. Because the slope of the curve between organism mass and $[\text{}^{63}\text{Cu}]_{\text{b,snail}}$ increased exponentially in organisms $<\sim 2$ mg, mass measurement errors of as little as ± 0.1 mg could result in the calculation of drastically different $^{63}\text{Cu}_{\text{accumulated}}$ values. Organism size and $^{63}\text{Cu}_{\text{accumulated}}$ exhibited a slightly negative linear relationship, even after I re-calculated my results using size-specific $[\text{}^{63}\text{Cu}]_{\text{b,snail}}$ values, despite past work concluding that those two parameters should be positively correlated for ^{63}Cu in pond snails. This apparent and unexpected trend may have resulted from uncertainty in my $^{63}\text{Cu}_{\text{accumulated}}$ results due to the aforementioned extreme slope of the $[\text{}^{63}\text{Cu}]_{\text{b,snail}}$ curve. Additionally, it is possible that the observed size-dependent $^{63}\text{Cu}_{\text{accumulated}}$ trend was the result of the smaller (<3 mg dry weight) snails preferentially eating feeding mats composed of mixtures of diatoms and NFP, and larger (>3 mg dry weight) snails avoiding those feeding mats. Such behavior in *L. stagnalis* has not been observed in other studies, to my knowledge. The underlying cause of this apparent behavior cannot be identified without further research.

Although I was able to generate equations that improved my ability to calculate AE in snails <2 mg, results of organism-size analyses suggest that data for organisms that small may not be reliable. Because of the challenges posed during data collection (e.g., accurate weighing, feces collection, etc.) and in generating a high-resolution curve for the calculation of size-specific $[\text{}^{63}\text{Cu}]_{\text{b,snail}}$, I recommend that reverse-labeling stable isotope experiments not be conducted using snails weighing <2 mg. Additionally, I recommend that bioavailability studies

only be performed on organisms developing at similar growth rates (i.e., hatched around the same date and grown to a similar size). Differences in growth rates could be an additional source of between-organism variability and may influence the degree of isotopic reversal observed in snails.

In seeking to expand the implications of this work to other bioavailability studies, I concluded that uncertainty in $^{63}\text{Cu}_{\text{accumulated}}$ calculated for snails <2 mg may be due to the combined effects of high metabolic activity,⁴ weakly exponential growth rate,⁵ and variable growth rates in experimental organisms. High metabolic activity and weakly exponential growth rates have been reported in snails in early post-hatching ontogeny (0-10 weeks after hatching, and ~ 0.4 -3 mg).⁶ The effects of variable growth rates on metal bioavailability, and on isotopic reversal, appear to remain unstudied. To determine organism-size constraints for general studies of bioavailability, I recommend that preliminary studies and research be performed to determine the size at which both feeding and growth rates stabilize in the organism of study.

3.2 Recommendations for future research

The possibilities for expanding upon this work are extensive. To continue to evaluate the effects of MIW remediation on metal bioavailability, the adaptation of the methods used herein to species more ecologically relevant to high-gradient montane streams will be beneficial.

Possible species for this work could include midges (*Chironomidae*) or mayflies (*Ephemeroptera*). Potential issues in calculating ^{63}Cu accumulation while working with either of these types of organisms may include feces collection and the determination of accurate of $[\text{}^{63}\text{Cu}]_{\text{b,organism}}$, due to the small size of the organisms.

In addition to adapting these methods to other species, investigations of metal bioavailability for other metals of concern in NFCC will help to improve understanding of the

responses of MIW to treatment. Possible metals of interest for these future experiments may include aluminum (Al), cadmium (Cd), manganese (Mn), and zinc (Zn). Furthermore, metal bioavailability experiments using cobble in MIW pre- and post-remediation should be performed in more streams and regions, as well as in systems being remediated by other means (e.g., permeable reactive barriers, artificial wetlands, in situ methods, etc.). Expansion of this type of work to more systems will lead to a greater understanding of toxicological responses of MIW to remediation.

Although the results of my organism-size analyses are intriguing, further work is needed to fully determine the significance of the trends herein observed. To determine whether or not the observed relationships between organism size, Cu accumulation, and tissue Cu concentrations are unique to Cu in *L. stagnalis*, similar analyses using other metals and other organisms will need to be performed. Depending on the outcomes of such experiments, my results may have broader implications for the determination of organism-size limits in assessments of bioavailability.

Additional work in determining the biological cause of the observed organism-size trends may help to understand metal accumulation, storage, and metabolism in *L. stagnalis*. One possible approach to this type of work would be to conduct a similar experiment to that of Abbe et al.,⁷ in which the authors dissected oysters that had been exposed to dissolved aluminum (Al) to identify Al storage sites. The authors also examined specific mechanisms by which the oysters regulated tissue Al concentrations.

Finally, the contribution of ⁶³Cu in cobble and lettuce not expelled from snails' guts during the depuration period to total ⁶³Cu measured in digested samples should be explored. Any additional ⁶³Cu from food remaining in small organisms could result in seemingly high

[⁶³Cu]_{snail}. During this and other experiments (Appendix A: Supplemental Information), several organisms were not used to calculate AE due to their having excessively high [⁶³Cu]_{snail}. While we initially assumed these organisms to be outliers, their high values may have been the result of diatoms, cobble coatings, or lettuce not being expelled from organisms' guts during the depuration period. In an effort to isolate ⁶³Cu in gut contents, and not accumulated in snails' soft tissue, members of the Ranville Research Group will be working to identify elemental signatures that are unique to cobble coatings, diatoms, and lettuce. If unique elemental signatures can be identified for each of those components, calculations will be altered so that residual gut contents are not factored into values for accumulated ⁶³Cu.

3.3 References

- (1) *Liquid assets 2000: America's water resources at a turning point*; Technical Report EPA-840-B-00-001; United States Environmental Protection Agency: Washington, DC, 2000; <https://nepis.epa.gov/Exe/ZyPDF.cgi/20004GRW.PDF?Dockey=20004GRW.PDF>.
- (2) *Grand Opening Fact Sheet: Central City/Clear Creek Superfund Site*; Colorado Department of Public Health and Environment, Denver, CO, 2017.
- (3) Croteau, M.-N.; Cain, D. J.; Fuller, C. C. Novel and nontraditional use of stable isotope tracers to study metal bioavailability from natural particles. *Environ. Sci. Technol.* **2013**, *47*, 3424-3431; DOI 10.1021/es4000162f.
- (4) Williamson, P. Variables affecting body burdens of lead, zinc, and cadmium in a roadside population of the snail *Capaea hortensis* Müller. *Oecologia.* **1980**, *44* (2), 213-220; DOI 10.1007/BF00572682.
- (5) Zotin, A. A. Individual growth of *Lymnaea stagnalis* (Lymnaeidae, Gastropoda): II. late postlarval ontogeny. *Biol. Bull.* **2009**, *36* (6), 591-597; DOI 10.1134/S1062359009060077.
- (6) Zotin, A. A. The growth and energy metabolism of *Lymnaea stagnalis* (Lymnaeidae, Gastropoda): I. early postlarval period. *Biol. Bull.* **2009**, *36* (5), 455-463. DOI 10.1134/S1062359009050057.
- (7) Abbe, G. R.; Sanders, J. G.; Riedel, G. F. Silver uptake by the oyster (*Crassostrea virginica*): Effect of organism size and storage sites. *Estuarine, Coastal Shelf Sci.* **1994**, *39* (3), 249-260; DOI 10.1006/ecss.1994.1062.

APPENDIX A

SUPPORTING INFORMATION

A.1 Copper bioavailability data pre- and post-remediation

Table A.1 Summary of data used to determine Cu bioavailability in *L. stagnalis* not exposed to any material (B), exposed to diatoms only (D), and exposed to metal-oxyhydroxide cobble coatings removed from NFCC cobble collected in February 2017 (2/17) and August 2017 (8/17). Organisms found to have negative values for $^{63}\text{Cu}_{\text{accumulated}}$ were not included in final calculations of assimilation efficiency (AE).

Category	M_{snail} (mg)	$[^{63}\text{Cu}]_{\text{snail}}$ ($\mu\text{g } ^{63}\text{Cu g}_{\text{snail}}^{-1}$)	$[^{65}\text{Cu}]_{\text{snail}}$ ($\mu\text{g } ^{65}\text{Cu g}_{\text{snail}}^{-1}$)	$^{65}\text{Cu}:^{63}\text{Cu}$	$^{63}\text{Cu}_{\text{accumulated}}$ (ng)	AE (%)
B	1.07	59.15	109.86	1.9	-	-
B	0.93	67.91	85.08	1.3	-	-
B	0.81	76.90	123.24	1.6	-	-
B	1.2	56.56	79.03	1.4	-	-
B	0.98	57.09	44.00	0.8	-	-
B	3.08	34.37	138.94	4.0	-	-
B	1.06	61.98	78.52	1.3	-	-
B	1.05	63.23	129.00	2.0	-	-
B	2.41	43.39	126.54	2.9	-	-
B	4.95	35.90	149.99	4.2	-	-
B	1.83	42.21	106.64	2.5	-	-
B	0.52	118.30	182.95	1.5	-	-
B	1.21	56.31	115.66	2.1	-	-
B	0.41	155.18	219.81	1.4	-	-
B	0.52	104.67	63.25	0.6	-	-
B	0.63	97.92	139.40	1.4	-	-

Table A.1: Continued

Category	M _{snail} (mg)	[⁶³ Cu] _{snail} (μg ⁶³ Cu g _{snail} ⁻¹)	[⁶⁵ Cu] _{snail} (μg ⁶⁵ Cu g _{snail} ⁻¹)	⁶⁵ Cu: ⁶³ Cu	⁶³ Cu _{accumulated} (ng)	AE (%)
B	0.63	95.93	102.18	1.1	-	-
B	0.39	141.83	61.11	0.4	-	-
B	0.44	126.39	93.00	0.7	-	-
B	1.1	62.90	122.05	1.9	-	-
D	1.34	65.02	96.98	1.5	-	-
D	0.73	137.01	213.62	1.6	-	-
D	3.81	50.51	87.29	1.7	-	-
D	0.2	370.62	533.67	1.4	-	-
D	1.21	42.06	6.24	0.1	-	-
D	0.35	156.66	60.93	0.4	-	-
D	0.61	104.14	84.25	0.8	-	-
D	1.12	73.08	156.69	2.1	-	-
D	4.56	35.15	63.25	1.8	-	-
D	1.54	54.56	73.20	1.3	-	-
D	1.06	77.27	124.78	1.6	-	-
D	0.36	148.75	51.33	0.3	-	-
D	0.51	120.21	102.04	0.8	-	-
D	0.47	104.12	12.43		-	-
D	2.14	26.80	13.63	0.5	-	-
D	3.48	34.02	66.27	1.9	-	-
D	4.49	31.09	91.21	2.9	-	-
D	1.93	77.41	268.39	3.5	-	-

Table A.1: Continued

Category	M _{snail} (mg)	[⁶³ Cu] _{snail} (μg ⁶³ Cu g _{snail} ⁻¹)	[⁶⁵ Cu] _{snail} (μg ⁶⁵ Cu g _{snail} ⁻¹)	⁶⁵ Cu: ⁶³ Cu	⁶³ Cu _{accumulated} (ng)	AE (%)
2/17	0.48	206.27	302.87	1.5	73.27	58.91
2/17	5.02	11.55	4.85	0.4	-17.70	-41.67
2/17	1.2	186.54	298.84	1.6	113.41	29.91
2/17	1.78	48.79	55.70	1.1	-7.88	-2.01
2/17	1.73	66.32	127.28	1.9	8.60	13.00
2/17	0.96	127.15	195.25	1.5	42.59	16.46
2/17	0.57	146.31	162.39	1.1	27.47	31.53
2/17	3.59	17.65	13.32	0.8	-18.51	- 129.49
2/17	2.19	97.73	205.69	2.1	48.14	19.57
2/17	0.42	283.05	534.34	1.9	137.89	71.76
2/17	0.89	67.20	35.79	0.5	-21.63	- 208.49
2/17	3.15	24.46	25.35	1.0	-14.83	-57.37
2/17	2.66	71.82	129.15	1.8	28.05	15.90
2/17	1.26	122.67	235.91	1.9	51.81	31.63
2/17	3.7	28.57	43.89	1.5	-6.90	-6.96
2/17	2.05	100.39	223.38	2.2	48.65	22.03
2/17	0.54	247.06	431.62	1.7	123.94	48.05
2/17	0.27	233.23	251.15	1.1	39.18	52.68
8/17	0.98	55.99	22.66	0.4	-27.43	-95.72
8/17	4.37	15.50	11.39	0.7	-16.43	-25.67
8/17	2.17	113.80	256.86	2.3	63.93	22.77

Table A.1: Continued

Category	M _{snail} (mg)	[⁶³ Cu] _{snail} ($\mu\text{g } ^{63}\text{Cu g}_{\text{snail}}^{-1}$)	[⁶⁵ Cu] _{snail} ($\mu\text{g } ^{65}\text{Cu g}_{\text{snail}}^{-1}$)	⁶⁵ Cu: ⁶³ Cu	⁶³ Cu _{accumulated} (ng)	AE (%)
8/17	1.14	126.27	215.79	1.7	50.66	31.57
8/17	0.99	74.53	68.51	0.9	-8.35	1.80
8/17	3.6	22.63	24.36	1.1	-13.46	-8.16
8/17	1.51	126.20	262.07	2.1	63.18	28.04
8/17	0.57	209.71	348.67	1.7	90.88	58.26
8/17	3.17	23.85	18.96	0.8	-15.28	-97.93
8/17	0.44	478.79	1168.39	2.4	337.99	61.33
8/17	0.77	81.52	45.99	0.6	-16.11	-4.30
8/17	1.16	75.22	108.78	1.4	0.46	11.78
8/17	2.15	40.54	47.26	1.2	-9.63	-15.10
8/17	3.17	46.79	93.71	2.0	7.66	3.30
8/17	5.86	34.89	69.84	2.0	8.34	1.61
8/17	1.48	235.92	452.23	1.9	172.08	20.18
8/17	0.96	132.02	195.59	1.5	47.46	5.17
*8/17	0.32	-	-	-	-	-

*Organism was dead at the end of the dietborne exposure and was neither analyzed nor included in final calculations

Table A.2 Size-specific pre-exposure tissue concentrations of ⁶³Cu in *L. stagnalis* ([⁶³Cu]_{b,snail}) calculated using the equation of the curve fit to measured [⁶³Cu]_{snail} in “background” snails, and the difference between size-specific values and the average of all measured [⁶³Cu]_{snail} in “background” snails ($\overline{[^{63}\text{Cu}]_b}$). Positive differences are highlighted in green, and negative differences are highlighted in red.

M _{snail} (mg)	Size-specific [⁶³ Cu] _{b,snail} ($\mu\text{g } ^{63}\text{Cu g}_{\text{snail}}^{-1}$)	[⁶³ Cu] _{b,snail} - $\overline{[^{63}\text{Cu}]_b}$
0.27	159.50	81.60
0.42	120.85	42.95
0.44	117.37	39.47

Table A.2: Continued

Msnail (mg)	Size-specific [⁶³ Cu] _{b,snail} (μg ⁶³ Cu g _{snail} ⁻¹)	[⁶³ Cu] _{b,snail} - [⁶³ Cu] _b
0.48	111.13	33.23
0.54	103.20	25.30
0.57	99.76	21.86
0.57	99.76	21.86
0.77	82.59	4.69
0.89	75.41	-2.49
0.96	71.91	-5.99
0.96	71.91	-5.99
0.98	70.98	-6.92
0.99	70.53	-7.37
1.14	64.55	-13.35
1.16	63.85	-14.05
1.2	62.51	-15.39
1.26	60.62	-17.28
1.48	54.79	-23.11
1.51	54.11	-23.79
1.73	49.68	-28.22
1.78	48.80	-29.10
2.05	44.65	-33.25
2.15	43.34	-34.56
2.17	43.09	-34.81
2.19	42.84	-35.06
2.66	37.92	-39.98
3.15	34.10	-43.80
3.17	33.96	-43.94
3.17	33.96	-43.94
3.59	31.41	-46.49
3.6	31.35	-46.55
3.7	30.82	-47.08
4.37	27.76	-50.14
5.02	25.44	-52.46
5.86	23.09	-54.81

A.2 Water chemistry data collected on cobble coating collection dates

Table A.3 Summary of water chemistry measured in the field and analytically on both cobble sampling dates (February 2, 2017 and August 29, 2017) at the Railless Below Plant (RBP) site. ICP-AES data represent total (unfiltered) metals concentrations in mg L⁻¹. Only pH was measured in the field in February 2017, while pH, alkalinity, conductivity, and stream temperature were measured in August 2017. DL = detection limit, BDL = below detection limit, NM = not measured.

		DL (mg L ⁻¹)	February 2, 2017	August 29, 2017
ICP-AES	Al 308.215-A	0.0205	0.4976	0.2305
		DL (mg L ⁻¹)	February 2, 2017	August 29, 2017
	As 188.979-A*	0.0047	BDL	0.0164
	B 249.772-R	0.0459	0.0876	0.0304
	Ba 233.527-A*	0.0001	0.0254	0.0298
	Be 313.107-R	0.0002	0.0011	BDL
	Ca 315.887-R*	0.0064	84.3306	115.5214
	Cd 214.440-A	0.0001	0.0065	0.0011
	Co 228.616-A	0.0002	0.0302	NM
	Cr 205.560-A	0.0003	BDL	0.0012
	Cu 324.752-A	0.0011	0.1306	0.0465
	Fe 238.204-A	0.0003	22.8127	0.2744
	K 766.490-R	0.0323	3.8083	3.7334
	Li 670.784-R	0.0014	0.0173	0.0133
	Mg 279.553-R	0.0001	25.8366	24.2362
	Mg 285.213-R	0.0014	26.0374	24.0578
	Mn 257.610-A*	0.0000	6.5174	0.6202
	Na 589.592-R	0.1345	33.4076	26.1344
Ni 231.604-A	0.0005	0.0610	0.0046	

Table A.3: Continued

	DL (mg L ⁻¹)	February 2, 2017	August 29, 2017	
P 177.434-A	0.0106	0.0190	BDL	
Pb 220.353-A	0.0020	0.0183	0.0072	
S 180.669-A	0.0276	126.8980	128.4750	
Se 196.026-A	0.0100	BDL	BDL	
Si 251.611-A*	0.0114	8.6130	5.5659	
Sr 407.771-R*	0.0001	0.5691	0.5629	
Tl 190.801-A	0.0018	BDL	BDL	
V 292.402-A*	0.0008	0.0052	BDL	
Zn 213.857-A	0.0003	2.3960	0.4645	
Sn 189.927	0.0017	BDL	0.5629	
Mo 202.031	0.0010	BDL	0.0031	
Sb 217.582	0.0051	BDL	BDL	
Ti 334.940	0.0002	BDL	BDL	
Field Measurements	pH	-	7.2	7.6
	Alkalinity (mg L ⁻¹ as CaCO ₃)	-	NM	24
	Conductivity (μS cm ⁻¹)	-	NM	696
	Stream Temperature (°C)	-	NM	14.3

A.3 Single-timepoint copper bioavailability

A.3.1 Methods

A.3.1.1 Test organisms

Test organisms for single-timepoint bioavailability experiments were prepared according to the procedure outlined for the dual-timepoint bioavailability experiment, with the exception that organisms had masses of 0.7 ± 0.4 for the May 2017 armored coating experiment and 0.9 ± 0.9 for the August 2017 armored coating experiment (average mg dry weight \pm SD).

A.3.1.2 Feeding mats

Feeding mats for single-timepoint bioavailability experiments were prepared in the same manner as mats used for the dual-timepoint experiment. For both the May and August 2017 armored coating experiments, varying volumes of NFPS were used to create feeding mats having target total Cu concentrations of 0, 300, 600, 900, and 1200 $\mu\text{g Cu g}_{\text{mat}}^{-1}$ (g Cu + g diatom).

A.3.1.3 Bioavailability experiments

For the May and August 2017 armored coating experiments, 8 test organisms were placed in each of the 6 feeding cups and allowed to graze for 3-4 h. Additionally, 8 “background” snails were removed from the aquarium and immediately frozen to be prepared for analysis.

A.3.2 Results and discussion

A.3.2.1 Copper bioavailability in May 2017 armored NFCC cobble coatings

Calculated assimilation efficiencies (AE) in snails exposed to armored metal-oxyhydroxide cobble coatings collected from NFCC in May 2017 were highly variable across the range of Cu concentrations (Figure A.1). AE values, reported as $\text{AE} \pm 95\%$ confidence, ranged between $5.3\% \pm 6.43\%$ for $397 \mu\text{g } ^{63}\text{Cu g}^{-1}$ food and $56.6\% \pm 0\%$ for $256 \mu\text{g } ^{63}\text{Cu g}^{-1}$ food. Statistical power to determine AE values for each Cu concentration was limited due to the large number of organisms calculated to have had negative ^{63}Cu accumulation over the exposure

period. Negative ^{63}Cu accumulation in an organism indicates that the organism did not eat over the exposure period, therefore results of this experiment suggest that most organisms exposed to the May 2017 armored metal-oxyhydroxide cobble coatings did not eat a detectable amount of material. Low calculated ingestion rates (IR) in many organisms suggest that organisms may not have been eating during the exposure due to their experiencing the effects of Cu toxicity. The use of very small organisms in this experiment (0.7 ± 0.4 mg dry weight per individual \pm SD) may explain the observance of toxic effects in organisms at lower-than-expected Cu concentrations. Overall AE for armored metal-oxyhydroxide cobble coatings collected from NFCC in May 2017 was $67.0\%\pm 14.7\%$ (average AE \pm 95% confidence).

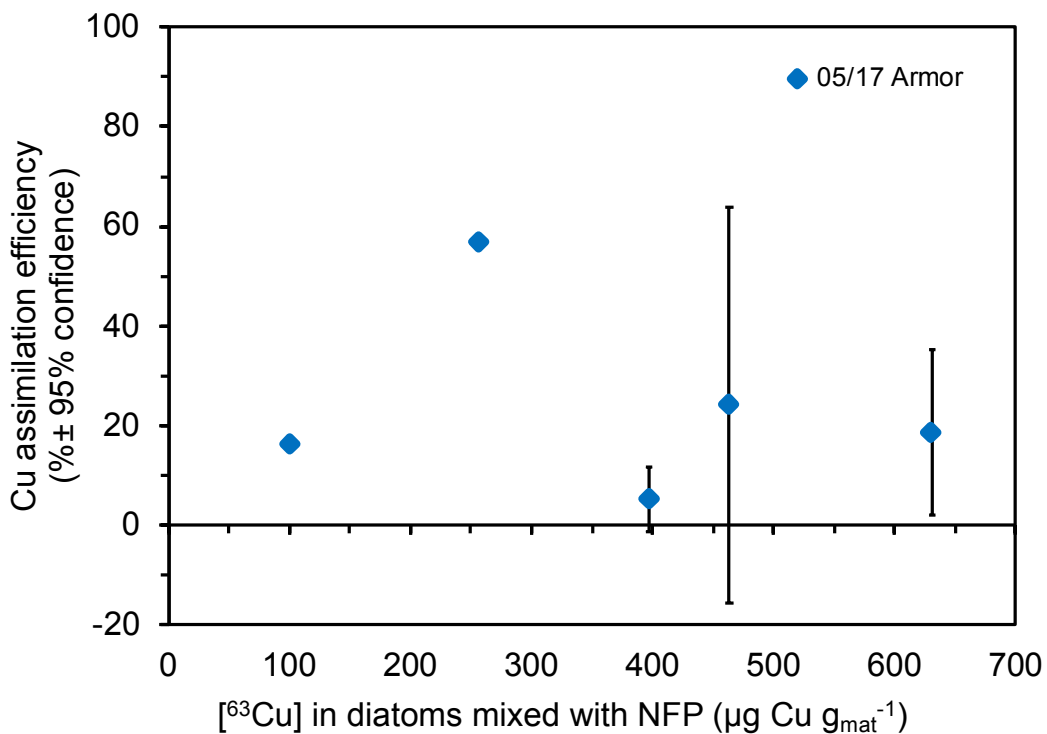


Figure A.1 Assimilation efficiency (AE) of ^{63}Cu by *L. stagnalis* exposed to mixtures of diatoms and armored metal-oxyhydroxide cobble coating particles removed from North Fork Clear Creek (NFC) cobble collected in May 2017. Diatom-particle feeding mats were prepared for target total [Cu] of 0, 300, 600, 900, and 1200 $\mu\text{g Cu g}^{-1}$ food. Error bars represent a 95% confidence interval.

A.3.2.2 Copper bioavailability in August 2017 armored NFCC cobble coatings

AE values calculated for snails exposed to armored metal-oxyhydroxide cobble coatings collected from NFCC in August 2017 ranged between $34.9\% \pm 7.4\%$ for food having $379 \mu\text{g } ^{63}\text{Cu g}^{-1}$ food and $42.9\% \pm 10.2\%$ for food with $631 \mu\text{g } ^{63}\text{Cu g}^{-1}$ food (Figure A.2). The overall range of AE values was much smaller than the resulting range in the May 2017 armor experiment, which may have been due, in part, to more organisms accumulating a detectable amount of ^{63}Cu over the exposure period. The inclusion of data for more organisms in AE calculations increased our statistical power, and may have improved overall results. It is unclear whether more organisms

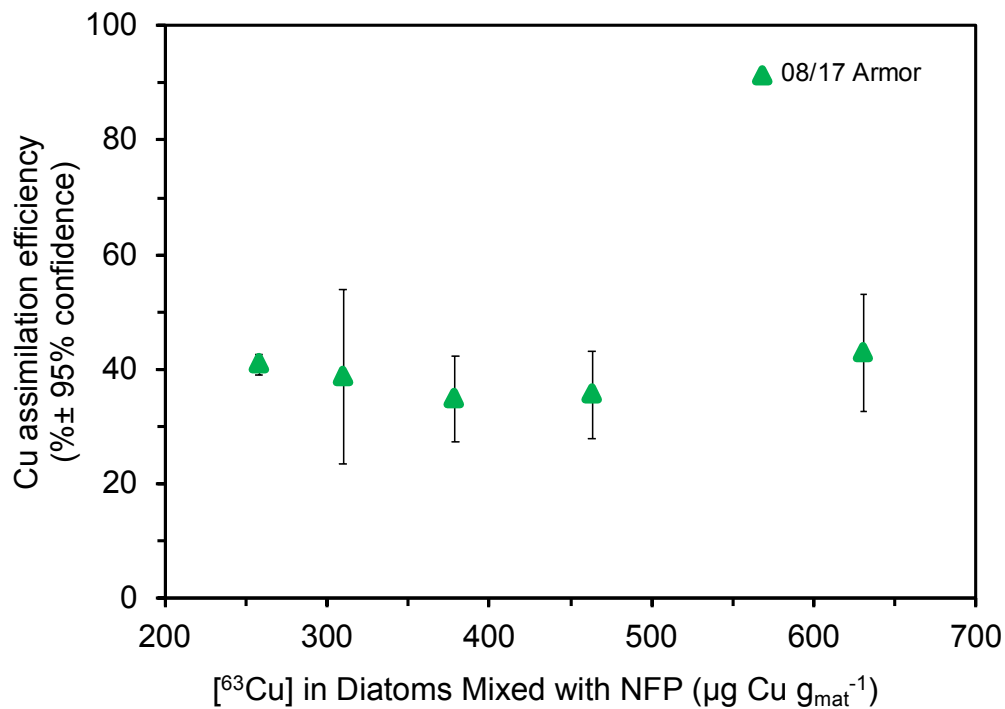


Figure A.2 Assimilation efficiency (AE) of ^{63}Cu by *L. stagnalis* exposed to mixtures of diatoms and armored metal-oxyhydroxide cobble coating particles removed from North Fork Clear Creek (NFC) cobble collected in August 2017. Diatom-particle feeding mats were prepared for target total [Cu] of 0, 300, 600, 900, and 1200 $\mu\text{g Cu g}^{-1}$ food. Error bars represent a 95% confidence interval.

ate a detectable amount during the exposure period because the material was, for unknown reasons, more appealing to the snails, or because the organisms were slightly larger (0.9 ± 0.9 mg dry weight) than those used during the May 2017 metal-oxyhydroxide cobble coating exposure. Overall AE for August 2017 armored metal-oxyhydroxide cobble coatings was $38.7\% \pm 3.1\%$ (average AE \pm 95% confidence).

A.3.2.3 Effect of size on ^{63}Cu accumulation

In order to investigate the effects of organism size on ^{63}Cu accumulation, we performed an experiment using the methods of Croteau et al.¹ in which freshwater snails (*Lymnaea stagnalis*) spanning a large size range were exposed to loose metal-oxyhydroxide flocculent removed from North Fork Clear Creek (NFCC) cobble collected in May 2017. Results identified a positive correlation between organism mass and ^{63}Cu accumulation from NFCC metal-oxyhydroxide cobble coatings (Figure A.1). Organism sizes (mg dry weight \pm SD) and average ^{63}Cu accumulated over a 4-hour exposure period (ng \pm SD) are summarized in Table A.1.

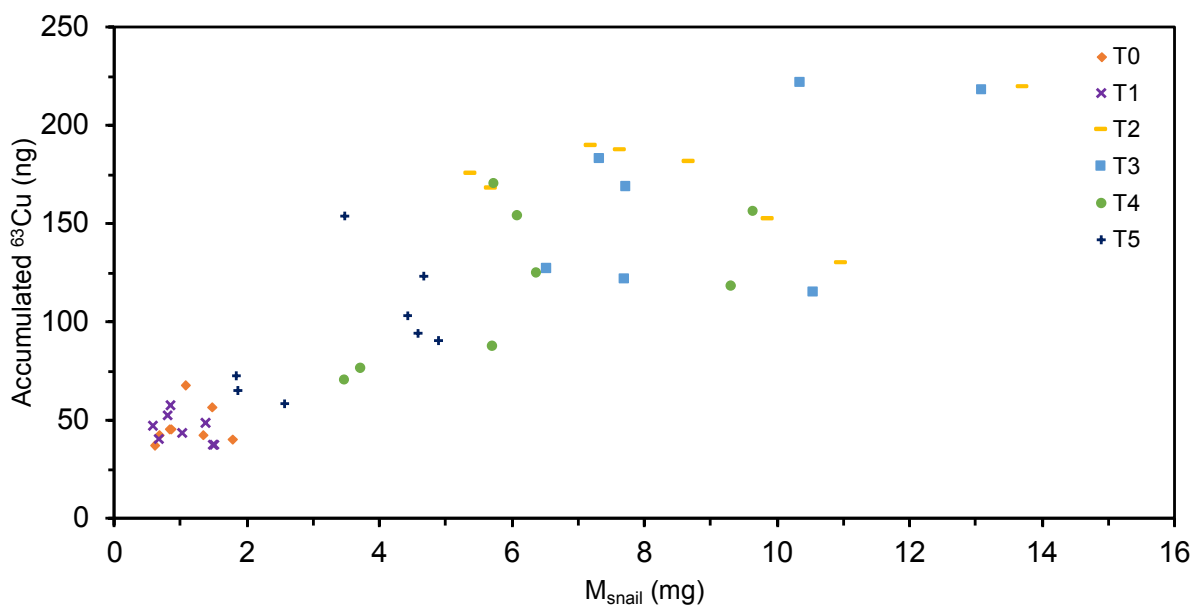


Figure A.3 ^{63}Cu accumulated over a 4-hour exposure period from loose metal-oxyhydroxide cobble coatings collected in May 2017 vs. organism dry tissue mass (mg)